DESY 15–077
DO–TH 15/07
MITP/15-039
August 2015

The $O(\alpha_s^3)$ Heavy Flavor Contributions to the Charged Current Structure Function $xF_3(x,Q^2)$ at Large Momentum Transfer

A. Behring[a], J. Blümlein[a], A. De Freitas[a,b], A. Hasselhuhn[c], A. von Manteuffel[d], and C. Schneider[b]

[a] *Deutsches Elektronen–Synchrotron, DESY, Platanenallee 6, D-15738 Zeuthen, Germany*

[b] *Research Institute for Symbolic Computation (RISC), Johannes Kepler University, Altenbergerstraße 69, A–4040, Linz, Austria*

[c] *Institute for Theoretical Particle Physics, Karlsruhe Institute of Technology (KIT) D-76128 Karlsruhe,*

[d] *PRISMA Cluster of Excellence, Institute of Physics, J. Gutenberg University, D-55099 Mainz, Germany.*

Abstract

We calculate the massive Wilson coefficients for the heavy flavor contributions to the non-singlet charged current deep-inelastic scattering structure function $xF_3^{W^+}(x,Q^2) + xF_3^{W^-}(x,Q^2)$ in the asymptotic region $Q^2 \gg m^2$ to 3-loop order in Quantum Chromodynamics (QCD) at general values of the Mellin variable N and the momentum fraction x. Besides the heavy quark pair production also the single heavy flavor excitation $s \to c$ contributes. Numerical results are presented for the charm quark contributions and consequences on the Gross-Llewellyn Smith sum rule are discussed.

1 Introduction

The non-singlet structure function $xF_3(x,Q^2)$ has been a first experimental source to determine the valence quark distributions $u_v(x,Q^2)$ and $d_v(x,Q^2)$ of the nucleon in deep-inelastic charged current neutrino-nucleon scattering [1–3]. Flavor non-singlet distributions allow for clear measurements of the strong coupling constant $a_s = \alpha_s/(4\pi) \equiv g_s^2/(4\pi)^2$ [4], due to the absence of gluonic effects in the QCD evolution [5].

Massless and massive QCD corrections have been calculated in Refs. [6–9] to first order in the strong coupling constant[1] and in Refs. [11–15] to $O(a_s^2)$[2]. The massive $O(a_s^2)$ corrections were calculated in the asymptotic representation [16], which is valid at high scales Q^2. One may perform an $O(a_s)$ comparison for the process of single heavy quark excitation. Here the approximation holds for $Q^2/m^2 \gtrsim 50$ [17], where $Q^2 = -q^2$ denotes the virtuality of the 4-momentum transfer q, and m is the heavy quark mass.

The present data on the neutrino structure function $xF_3(x,Q^2)$ or similar measurements at HERA [18] have not yet reached the level of precision of 1-2 %, as is the case for the structure function $F_2(x,Q^2)$ in neutral current deep-inelastic scattering. However, at neutrino factories planned for the future [19] this situation will change and even 3-loop QCD corrections will be of importance. The experimental precision reached for charged current interactions at the *ep* collider HERA can also be further refined at future high energy facilities probing deep-inelastic scattering, such as LHeC [20] and EIC [21]. It is expected that non-singlet data taken at these facilities will help to improve further the knowledge of the strong coupling constant $\alpha_s(M_Z^2)$ [22]. The 3-loop massless Wilson coefficient for the structure function combination $xF_3^{W^+}(x,Q^2) + xF_3^{W^-}(x,Q^2$ has been calculated in Ref. [23]. In the present paper we calculate the massive 3-loop Wilson coefficient for this combination in the asymptotic region $Q^2 \gg m^2$.

The charged current structure functions $xF_3^{W^\pm}(x,Q^2)$ may be measured both in neutrino- and charged lepton-nucleon scattering. In the case of single gauge boson exchange the differential scattering cross sections read [24, 25] :

$$\frac{d\sigma^{\nu(\bar{\nu})}}{dxdy} = \frac{G_F^2 s}{4\pi}\frac{M_W^4}{(M_W^2+Q^2)^2} \times\left\{\left(1+(1-y)^2\right)F_2^{W^\pm}(x,Q^2) - y^2 F_L^{W^\pm}(x,Q^2) \pm \left(1-(1-y)^2\right)xF_3^{W^\pm}(x,Q^2)\right\} \tag{1.1}$$

$$\frac{d\sigma^{l(\bar{l})}}{dxdy} = \frac{G_F^2 s}{4\pi}\frac{M_W^4}{(M_W^2+Q^2)^2} \times\left\{\left(1+(1-y)^2\right)F_2^{W^\mp}(x,Q^2) - y^2 F_L^{W^\mp}(x,Q^2) \pm \left(1-(1-y)^2\right)xF_3^{W^\mp}(x,Q^2)\right\}. \tag{1.2}$$

Here $x = Q^2/ys$ and $y = q.P/l.P$ denote the Bjorken variables, l and P are the incoming lepton and nucleon 4-momenta, and $s = (l+P)^2$. G_F is the Fermi constant and M_W the mass of the W-boson. $F_i^{W^\pm}(x,Q^2)$ are the structure functions, where the $+(-)$ signs refer to incoming neutrinos (antineutrinos) and charged antileptons (leptons), respectively. We will consider the combination of structure functions

$$xF_3^{W^+-W^-}(x,Q^2) = xF_3^{W^+}(x,Q^2) + xF_3^{W^-}(x,Q^2) \tag{1.3}$$

[1] The massive 1-loop corrections given in [10] were corrected in [8], see also [9].

[2] Some results given in [13] have been corrected in Ref. [14].

in the following. It can be measured projecting onto the kinematic factor $Y_- = 1-(1-y)^2$ of the differential cross sections at $x, Q^2 = \text{const.}$ as a difference. It is given by

$$\begin{aligned} F_3^{W^+-W^-}(x,Q^2) &= \Big[|V_{du}|^2(d-\overline{d}) + |V_{su}|^2(s-\overline{s}) + V_u(u-\overline{u})\Big] \otimes \Big[C_{q,3}^{W^+-W^-,\rm NS} + L_{q,3}^{W^+-W^-,\rm NS}\Big] \\ &+ \Big[|V_{dc}|^2(d-\overline{d}) + |V_{sc}|^2(s-\overline{s})\Big] \otimes H_{q,3}^{W^+-W^-,\rm NS} \;, \end{aligned} \tag{1.4}$$

with one massless Wilson coefficient $C_{q,3}^{W^+-W^-,\rm NS}$ and two massive Wilson coefficients $L_{q,3}^{W^+-W^-,\rm NS}$ and $H_{q,3}^{W^+-W^-,\rm NS}$, see Section 2. The coefficients V_{ij} are the Cabibbo-Kobayashi-Maskawa (CKM) [26, 27] matrix elements, where $V_u = |V_{du}|^2 + |V_{su}|^2$, and the present numerical values are [18]

$$|V_{du}| = 0.97425 \tag{1.5}$$
$$|V_{su}| = 0.2253 \tag{1.6}$$
$$|V_{dc}| = 0.225 \tag{1.7}$$
$$|V_{sc}| = 0.986 \;. \tag{1.8}$$

The massless Wilson coefficient reads to $O(a_s^3)$

$$C_{q,3}^{W^+-W^-,\rm NS}\left(x,\frac{Q^2}{\mu^2}\right) = \delta(1-x) + \sum_{k=1}^{3} a_s^k(\mu^2) C_{q,3}^{(k),W^+-W^-,\rm NS}\left(x,\frac{Q^2}{\mu^2}\right) \;, \tag{1.9}$$

where μ denotes both the factorization and renormalization scale, which have been set equal $\mu = \mu_R = \mu_F$[3], and

$$A(x) \otimes B(x) = \int_0^1 dx_1 \int_0^1 dx_2 \delta(x - x_1 x_2) A(x_1) B(x_2) \tag{1.10}$$

is the Mellin convolution. u, d and s are the light quark number densities and $\bar{q}$ denotes the corresponding antiquark densities, written here for a proton target. The valence distributions are given by

$$q_v = q - \bar{q} \;. \tag{1.11}$$

Very often one considers the case

$$s_v = 0 \;. \tag{1.12}$$

Various experiments are carried out using isoscalar targets, possessing neutron-proton symmetry. Here the following replacements have to be made

$$\begin{aligned} u &\to \tfrac{1}{2}(u+d), & \bar{u} &\to \tfrac{1}{2}\left(\bar{u}+\bar{d}\right) \\ d &\to \tfrac{1}{2}(u+d), & \bar{d} &\to \tfrac{1}{2}\left(\bar{u}+\bar{d}\right). \end{aligned} \tag{1.13}$$

The paper is organized as follows. In Section 2 we calculate the heavy flavor contributions to the non-singlet Wilson coefficients in the asymptotic region $Q^2 \gg m^2$ to the structure function $xF_3^{W^+-W^-}(x,Q^2)$ to 3-loop order in the strong coupling constant. We present the results both in Mellin N and x–space. Numerical results are given in Section 3. Consequences for the Gross-Llewellyn sum rule are discussed in Section 4, and Section 5 contains the conclusions. An appendix deals with a technical detail.

[3]For the scale dependence of the Wilson coefficient see e.g. [28].

2 The Wilson Coefficients

The asymptotic heavy flavor corrections to the structure function $xF_3^{W^+-W^-}(x,Q^2)$ are resulting from the Wilson coefficients $L_{q,3}^{W^+-W^-,\rm NS}$ and $H_{q,3}^{W^+-W^-,\rm NS}$. In the former case the charged current couples to a line of light quarks only, while in the latter case a heavy quark is excited by the exchanged W-boson with or without other heavy flavor effects through QCD corrections. In the following we work in Mellin space. The corresponding representation is obtained applying the transformation

$$\mathbf{M}[f(x)](N) = \int_0^1 dx x^{N-1} f(x) \tag{2.1}$$

to the above relations. One obtains

$$L_{q,3}^{W^+-W^-,\rm NS}(N_F+1) = A_{qq,Q}^{\rm NS} C_{q,3}^{W^+-W^-,\rm NS}(N_F+1) - C_{q,3}^{W^+-W^-,\rm NS}(N_F) \tag{2.2}$$

$$H_{q,3}^{W^+-W^-,\rm NS}(N_F+1) = A_{qq,Q}^{\rm NS} C_{q,3}^{W^+-W^-,\rm NS}(N_F+1) \tag{2.3}$$

as the general relations. Here $A_{qq,Q}^{\rm NS} \equiv A_{qq,Q}^{\rm NS}(N_F+1)$ denotes the massive non-singlet operator matrix element [29,30]. The expansion of both the massive operator matrix element (OME) and the massless Wilson coefficients in the strong coupling constant to 3-loop order leads to

$$\begin{aligned} L_{q,3}^{W^+-W^-,\rm NS}(N_F+1) &= a_s^2 A_{qq,Q}^{(2),\rm NS} + \hat{C}_{q,3}^{(2),W^+-W^-,\rm NS}(N_F) + a_s^3 \Bigg[A_{qq,Q}^{(3),\rm NS} \\ &\quad + A_{qq,Q}^{(2),\rm NS} C_{q,3}^{(1),W^+-W^-,\rm NS}(N_F+1) + \hat{C}_{q,3}^{(3),W^+-W^-,\rm NS}(N_F) \Bigg] , \end{aligned} \tag{2.4}$$

$$\begin{aligned} H_{q,3}^{W^+-W^-,\rm NS}(N_F+1) &= 1 + a_s C_{q,3}^{(1),W^+-W^-,\rm NS}(N_F+1) \\ &\quad + a_s^2 \left[A_{qq,Q}^{(2),\rm NS} + C_{q,3}^{(2),W^+-W^-,\rm NS}(N_F+1) \right] \\ &\quad + a_s^3 \Bigg[A_{qq,Q}^{(3),\rm NS} + A_{qq,Q}^{(2),\rm NS} C_{q,3}^{(1),W^+-W^-,\rm NS}(N_F+1) \\ &\quad + C_{q,3}^{(3),W^+-W^-,\rm NS}(N_F+1) \Bigg] \end{aligned} \tag{2.5}$$

$$= L_{q,3}^{W^+-W^-,\rm NS}(N_F+1) + C_{q,3}^{W^+-W^-,\rm NS}(N_F), \tag{2.6}$$

with $C_{q,3}^{W^+-W^-,\rm NS}(N_F)$ the massless Wilson coefficient up to 3-loop order. Here we use the convention

$$\hat{f}(N_F) = f(N_F+1) - f(N_F) \ . \tag{2.7}$$

The notation label 'N_F+1' in some of the above quantities means that they depend on N_F massless and one massive flavor.

The calculation of the different contributions to the Wilson coefficients (2.4, 2.5) is performed in $D = 4+\varepsilon$ dimensions to regulate the Feynman integrals. The treatment of γ_5 has to be considered. In the flavor non-singlet case both for the massive OMEs and the massless Wilson coefficients, γ_5 always appears in traces along one quark line. For the asymptotic Wilson coefficient $L_{q,3}^{\rm NS}$, this line is massless, while for $H_{q,3}^{\rm NS}$ also heavy quarks contribute due to single

charged current flavor excitations like $s \to c$. Still we are considering the case in which power corrections $(m^2/Q^2)^k,\ k \in \mathbb{N}, k \geq 1$, are disregarded and therefore the corresponding line has to be treated as massless. In this case a (reversed) Ward-Takahashi identity implies anti-commuting γ_5, mapping the corresponding vertex correction to a self-energy correction, which is the same in the case without γ_5.

The inclusive massive OME $A_{qq,Q}^{\rm NS}$ to 3-loop order for even and odd moments N has been calculated in Ref. [30]. The corresponding Feynman integrals have been reduced using integration-by-parts relations [31] applying an extension of the package `Reduze 2` [32][4]. The master integrals have been calculated using hypergeometric, Mellin-Barnes and differential equation techniques, mapping them to recurrences, which have been solved by modern summation technologies using extensively the packages `Sigma` [35, 36], `EvaluateMultiSums`, `SumProduction` [37], ρ`sum` [38], and `HarmonicSums` [39].

In Mellin N space the Wilson coefficient can be expressed by nested harmonic sums $S_{\vec{a}}(N)$ [40] which are defined by

$$S_{b,\vec{a}}(N) = \sum_{k=1}^{N} \frac{(\mathrm{sign}(b))^k}{k^{|b|}} S_{\vec{a}}(k), \quad S_\emptyset = 1,\ b, a_i \in \mathbb{Z}, b, a_i \neq 0, N > 0, N \in \mathbb{N}. \tag{2.8}$$

In the following, we drop the argument N of the harmonic sums and use the short-hand notation $S_{\vec{a}}(N) \equiv S_{\vec{a}}$. The Wilson coefficients depend on the logarithms

$$L_Q = \ln\left(\frac{Q^2}{\mu^2}\right) \qquad \text{and} \qquad L_M = \ln\left(\frac{m^2}{\mu^2}\right). \tag{2.9}$$

As a short-hand notation we define the leading order splitting function $\gamma_{qq}^{(0)}$ without its color factor

$$\gamma_{qq}^{(0)} = 4\left[2S_1 - \frac{3N^2+3N+2}{2N(N+1)}\right]. \tag{2.10}$$

The massive Wilson coefficient for the structure function $xF_3^{W^+-W^-}(x,Q^2)$ in the asymptotic region in the on-shell scheme in Mellin space is given by

$$\begin{aligned}
&L_{q,3}^{W^+-W^-,\rm NS}(N) = \\
&a_s^2 C_F T_F \Bigg\{ L_Q \left[-\frac{2P_9}{9N^2(N+1)^2} + \frac{4\big(29N^2+29N-6\big)}{9N(N+1)} S_1 + \frac{8}{3}S_1^2 - 8S_2 \right] \\
&+ L_M \left[\frac{2P_4}{9N^2(N+1)^2} - \frac{80}{9}S_1 + \frac{16}{3}S_2 \right] - \frac{\gamma_{qq}^{(0)} L_M^2}{3} - \frac{\gamma_{qq}^{(0)} L_Q^2}{3} + \frac{P_{35}}{27N^3(N+1)^3} \\
&+ \left(-\frac{2P_{14}}{27N^2(N+1)^2} + \frac{8}{3}S_2 \right) S_1 - \frac{2\big(29N^2+29N-6\big)}{9N(N+1)} S_1^2 - \frac{8}{9}S_1^3 \\
&+ \frac{2\big(35N^2+35N-2\big)}{3N(N+1)} S_2 - \frac{112}{9}S_3 + \frac{16}{3}S_{2,1} \Bigg\} + a_s^3 \Bigg\{ C_F^2 T_F \Bigg[\frac{1}{6}{\gamma_{qq}^{(0)}}^2 L_Q \big(L_Q^2 \\
&+ L_M^2\big) + L_M^2 \left[-\frac{2P_{29}}{3N^3(N+1)^3} + \frac{2P_8}{3N^2(N+1)^2} S_1 - \frac{4(N-1)(N+2)}{N(N+1)} S_1^2 \right. \\
&\left. - \frac{16}{3}S_1^3 + \frac{10}{3}\gamma_{qq}^{(0)} S_2 + \frac{64}{3}S_3 + \left(-\frac{64}{3N(N+1)} + \frac{128}{3}S_1 \right) S_{-2} + \frac{64}{3}S_{-3} \right.
\end{aligned}$$

[4]The package `Reduze 2` uses the packages `Fermat` [33] and `Ginac` [34].

$$
-\frac{128}{3}S_{-2,1}\Big] + L_Q^2\Big[-\frac{2P_{31}}{9N^3(N+1)^3} + \frac{2P_{15}}{9N^2(N+1)^2}S_1 - \frac{4\big(107N^2+107N-54\big)}{9N(N+1)}S_1^2
$$
$$
-16S_1^3 + \frac{22}{3}\gamma_{qq}^{(0)}S_2 + \frac{64}{3}S_3 + \left(-\frac{64}{3N(N+1)} + \frac{128}{3}S_1\right)S_{-2} + \frac{64}{3}S_{-3}
$$
$$
-\frac{128}{3}S_{-2,1}\Big] + \gamma_{qq}^{(0)}L_M L_Q\left[\frac{P_2}{9N^2(N+1)^2} + \frac{40}{9}S_1 - \frac{8}{3}S_2\right] + L_Q\Big[\frac{80}{9}S_1^4 + \frac{448}{3}S_{-4}
$$
$$
+\frac{4P_{50}}{27(N-1)N^4(N+1)^4(N+2)} + \left(-\frac{16\big(9N^2+9N-2\big)}{N(N+1)} + 64S_1\right)\zeta_3
$$
$$
+\left(-\frac{4P_{38}}{27N^3(N+1)^3} - \frac{32\big(67N^2+67N-21\big)}{9N(N+1)}S_2 + \frac{640}{9}S_3 + \frac{64}{3}S_{2,1} + \frac{512}{3}S_{-2,1}\right)S_1
$$
$$
+\left(\frac{2P_{18}}{27N^2(N+1)^2} - \frac{224}{3}S_2\right)S_1^2 + \frac{32(4N-1)(4N+5)}{9N(N+1)}S_1^3 + \frac{2P_{17}}{9N^2(N+1)^2}S_2
$$
$$
+48S_2^2 - \frac{32\big(53N^2+53N+16\big)}{9N(N+1)}S_3 + \frac{352}{3}S_4 + \Bigg(-\frac{64P_{28}}{9(N-1)N^2(N+1)^2(N+2)}
$$
$$
-\frac{128\big(10N^2+10N-3\big)}{9N(N+1)}S_1 - \frac{256}{3}S_1^2 + \frac{256}{3}S_2\Bigg)S_{-2} + 64S_{-2}^2 + 64S_{3,1}
$$
$$
+\left(-\frac{64\big(10N^2+10N+9\big)}{9N(N+1)} + \frac{256}{3}S_1\right)S_{-3} + \frac{16\big(9N^2+9N-2\big)}{3N(N+1)}S_{2,1}
$$
$$
+\frac{128\big(10N^2+10N-3\big)S_{-2,1}}{9N(N+1)} - \frac{256}{3}S_{-3,1} - 64S_{2,1,1} - \frac{512}{3}S_{-2,1,1}\Big]
$$
$$
+L_M\Big[\frac{P_{41}}{9N^4(N+1)^4} - 32S_2^2 + \left(\frac{2P_{32}}{9N^3(N+1)^3} + \frac{16\big(59N^2+59N-6\big)}{9N(N+1)}S_2 - \frac{256}{3}S_3\right.
$$
$$
\left.-\frac{256}{3}S_{-2,1}\right)S_1 + \left(-\frac{4P_6}{3N^2(N+1)^2} + \frac{32}{3}S_2\right)S_1^2 - \frac{160}{9}S_1^3 - \frac{4P_{11}}{9N^2(N+1)^2}S_2
$$
$$
+\frac{32\big(29N^2+29N+12\big)}{9N(N+1)}S_3 - \frac{256}{3}S_4 + \left(-\frac{64\big(16N^2+10N-3\big)}{9N^2(N+1)^2} + \frac{1280}{9}S_1\right.
$$
$$
\left.-\frac{128}{3}S_2\right)S_{-2} + \left(\frac{64\big(10N^2+10N+3\big)}{9N(N+1)} - \frac{128}{3}S_1\right)S_{-3} - \frac{128}{3}S_{-4} + \frac{128}{3}S_{3,1}
$$
$$
-\frac{128\big(10N^2+10N-3\big)}{9N(N+1)}S_{-2,1} - \frac{128}{3}S_{-2,2} + \frac{512}{3}S_{-2,1,1} + 8\gamma_{qq}^{(0)}\zeta_3\Big]
$$
$$
+\frac{P_{48}}{162N^5(N+1)^5} - \frac{128\big(112N^3+112N^2-39N+18\big)}{81N^2(N+1)}S_{-2,1}
$$
$$
+\left(\frac{2P_{16}}{9N^2(N+1)^2} - \frac{1208}{9}S_1 - \frac{64}{3}S_2\right)\zeta_3 + \gamma_{qq}^{(0)}\left(-\frac{8B_4}{3} + 12\zeta_4 + \frac{8}{3}S_{2,1,1}\right)
$$
$$
+\Bigg(\frac{P_{47}}{162N^4(N+1)^4} + \frac{8P_{19}}{81N^2(N+1)^2}S_2 - \frac{64}{9}S_2^2 - \frac{8\big(347N^2+347N+54\big)S_3}{27N(N+1)}
$$
$$
+\frac{704}{9}S_4 + \frac{128}{9N(N+1)}S_{2,1} - \frac{320}{9}S_{3,1} - \frac{256\big(10N^2+10N-3\big)}{27N(N+1)}S_{-2,1} - \frac{256}{9}S_{-2,2}
$$
$$
+\frac{1024}{9}S_{-2,1,1}\Bigg)S_1 + \left(\frac{P_{26}}{9N^3(N+1)^3} + \frac{16\big(5N^2+5N-4\big)}{9N(N+1)}S_2 + 16S_3 - \frac{128}{9}S_{2,1}\right.
$$

$$
-\frac{256}{9}S_{-2,1}\Big)S_1^2+\Big(-\frac{16P_7}{27N^2(N+1)^2}+\frac{128}{27}S_2\Big)S_1^3+\Big(\frac{P_{25}}{81N^3(N+1)^3}+\frac{400}{27}S_3
$$
$$
+\frac{256}{3}S_{-2,1}\Big)S_2-\frac{32\big(23N^2+23N-3\big)}{27N(N+1)}S_2^2+\frac{8P_{20}}{81N^2(N+1)^2}S_3+\frac{512}{9}S_5
$$
$$
-\frac{176\big(17N^2+17N+6\big)}{27N(N+1)}S_4+\Big(-\frac{64P_{12}}{81N^3(N+1)^3}+\frac{128P_{10}}{81N^2(N+1)^2}S_1-\frac{1280}{27}S_2
$$
$$
-\frac{128}{9N(N+1)}S_1^2+\frac{256}{27}S_1^3+\frac{512}{27}S_3-\frac{512}{9}S_{2,1}\Big)S_{-2}+\Big(-\frac{128\big(10N^2+10N+3\big)}{27N(N+1)}S_1
$$
$$
+\frac{64\big(112N^3+224N^2+169N+39\big)}{81N(N+1)^2}+\frac{128}{9}S_1^2+\frac{128}{9}S_2\Big)S_{-3}+\Big(\frac{256}{9}S_1
$$
$$
-\frac{128\big(10N^2+10N+3\big)}{27N(N+1)}\Big)S_{-4}+\frac{256}{9}S_{-5}+\frac{16P_5S_{2,1}}{9N^2(N+1)^2}+\frac{256}{9}S_{2,3}-\frac{512}{9}S_{2,-3}
$$
$$
+\frac{16\big(89N^2+89N+30\big)}{27N(N+1)}S_{3,1}-\frac{512}{9}S_{4,1}-\frac{128\big(10N^2+10N-3\big)}{27N(N+1)}S_{-2,2}
$$
$$
+\frac{256}{9}\big(2S_{-2,3}+2S_{2,1,-2}+S_{3,1,1}+2S_{-2,2,1}\big)+\frac{512\big(10N^2+10N-3\big)}{27N(N+1)}S_{-2,1,1}
$$
$$
-\frac{2048}{9}S_{-2,1,1,1}\Bigg]
$$
$$
+C_AC_FT_F\Bigg[\frac{22\gamma_{qq}^{(0)}}{27}\left(L_M^3+2L_Q^3\right)+L_M^2\Bigg[\frac{\gamma_{qq}^{(0)}P_1}{9N^2(N+1)^2}-\frac{16P_3}{3N^2(N+1)^2}S_1-\frac{32}{3}S_3
$$
$$
+\Big(\frac{32}{3N(N+1)}-\frac{64}{3}S_1\Big)S_{-2}-\frac{32}{3}S_{-3}+\frac{64}{3}S_{-2,1}\Bigg]+L_Q^2\Bigg[\frac{2P_{37}}{27N^3(N+1)^3}
$$
$$
-\frac{16\big(194N^2+194N-33\big)}{27N(N+1)}S_1-\frac{176}{9}S_1^2+\frac{176}{3}S_2-\frac{32}{3}S_3+\Big(\frac{32}{3N(N+1)}
$$
$$
-\frac{64}{3}S_1\Big)S_{-2}-\frac{32}{3}S_{-3}+\frac{64}{3}S_{-2,1}\Bigg]+L_M\Bigg[\frac{P_{40}}{81N^4(N+1)^4}+\Big(-\frac{8P_{30}}{81N^3(N+1)^3}
$$
$$
+32S_3+\frac{128}{3}S_{-2,1}\Big)S_1+\frac{1792}{27}S_2-\frac{16\big(31N^2+31N+9\big)}{9N(N+1)}S_3+\frac{160}{3}S_4
$$
$$
+\Big(\frac{32\big(16N^2+10N-3\big)}{9N^2(N+1)^2}-\frac{640}{9}S_1+\frac{64}{3}S_2\Big)S_{-2}+\Big(-\frac{32\big(10N^2+10N+3\big)}{9N(N+1)}
$$
$$
+\frac{64}{3}S_1\Big)S_{-3}+\frac{64}{3}S_{-4}-\frac{128}{3}S_{3,1}+\frac{64\big(10N^2+10N-3\big)}{9N(N+1)}S_{-2,1}+\frac{64}{3}S_{-2,2}
$$
$$
-\frac{256}{3}S_{-2,1,1}-8\gamma_{qq}^{(0)}\zeta_3\Bigg]+L_Q\Bigg[-\frac{16\big(230N^3+460N^2+213N-11\big)}{9N(N+1)^2}S_2
$$
$$
-\frac{4P_{51}}{81(N-1)N^4(N+1)^4(N+2)}+\Big(\frac{4P_{39}}{81N^3(N+1)^3}-\frac{32\big(11N^2+11N+3\big)}{9N(N+1)}S_2
$$
$$
+32S_3-\frac{128}{3}S_{2,1}-\frac{256}{3}S_{-2,1}\Big)S_1+\Big(\frac{16\big(194N^2+194N-33\big)}{27N(N+1)}+\frac{32}{3}S_2\Big)S_1^2
$$
$$
+\frac{352}{27}S_1^3-\frac{32}{3}S_2^2+\frac{16\big(368N^2+368N-9\big)}{27N(N+1)}S_3+\Big(\frac{32P_{28}}{9(N-1)N^2(N+1)^2(N+2)}
$$

$$+\frac{64\big(10N^2+10N-3\big)}{9N(N+1)}S_1+\frac{128}{3}S_1^2-\frac{128}{3}S_2\Big)S_{-2}-\frac{224}{3}S_4-32S_{-2}^2$$
$$+\Big(\frac{32\big(10N^2+10N+9\big)}{9N(N+1)}-\frac{128}{3}S_1\Big)S_{-3}-\frac{224}{3}S_{-4}-\frac{64\big(11N^2+11N-3\big)}{9N(N+1)}S_{2,1}$$
$$-\frac{64}{3}S_{3,1}-\frac{64\big(10N^2+10N-3\big)}{9N(N+1)}S_{-2,1}+\frac{128}{3}S_{-3,1}+64S_{2,1,1}+\frac{256}{3}S_{-2,1,1}$$
$$+\Big(96-64S_1\Big)\zeta_3\Big]+\frac{P_{49}}{729N^5(N+1)^5}+\frac{S_{-2,1}}{N^2(N+1)}\frac{64}{81}\big(112N^3+112N^2-39N$$
$$+18\big)+\Big(\frac{P_{24}}{27N^2(N+1)^2}+\frac{4\big(593N^2+593N+108\big)}{27N(N+1)}S_1-16S_1^2+16S_2\Big)\zeta_3$$
$$+\gamma_{qq}^{(0)}\Big(\frac{4B_4}{3}-12\zeta_4-4S_{2,1,1}\Big)+\Big(-\frac{4P_{46}}{729N^4(N+1)^4}-\frac{16(N-1)}{9N^2(N+1)^2}S_2$$
$$\times\big(2N^3-N^2-N-2\big)+\frac{112}{9}S_2^2+\frac{80(2N+1)^2S_3}{9N(N+1)}-\frac{208}{9}S_4+\frac{64}{3}S_{3,1}+\frac{128}{9}S_{-2,2}$$
$$-\frac{8\big(9N^2+9N+16\big)}{9N(N+1)}S_{2,1}+\frac{128\big(10N^2+10N-3\big)}{27N(N+1)}S_{-2,1}-\frac{512}{9}S_{-2,1,1}\Big)S_1$$
$$+\Big(\frac{4P_{21}}{9N^3(N+1)^3}+\frac{32}{9N(N+1)}S_2-\frac{80}{9}S_3+\frac{128}{9}S_{2,1}+\frac{128}{9}S_{-2,1}\Big)S_1^2+\Big(\frac{496}{27}S_3$$
$$+\frac{4P_{36}}{81N^3(N+1)^3}-\frac{64}{3}S_{2,1}-\frac{128}{3}S_{-2,1}\Big)S_2-\frac{64}{27}S_1^3S_2-\frac{4\big(15N^2+15N+14\big)}{9N(N+1)}S_2^2$$
$$-\frac{8P_{23}}{81N^2(N+1)^2}S_3+\frac{4\big(443N^2+443N+78\big)}{27N(N+1)}S_4-\frac{224}{9}S_5+\Big(\frac{32P_{12}}{81N^3(N+1)^3}$$
$$-\frac{64P_{10}}{81N^2(N+1)^2}S_1+\frac{64}{9N(N+1)}S_1^2-\frac{128}{27}S_1^3+\frac{640}{27}S_2-\frac{256}{27}S_3+\frac{256}{9}S_{2,1}\Big)S_{-2}$$
$$+\Big(-\frac{32\big(112N^3+224N^2+169N+39\big)}{81N(N+1)^2}+\frac{64\big(10N^2+10N+3\big)}{27N(N+1)}S_1$$
$$-\frac{64}{9}S_1^2-\frac{64}{9}S_2\Big)S_{-3}+\Big(\frac{64\big(10N^2+10N+3\big)}{27N(N+1)}-\frac{128}{9}S_1\Big)S_{-4}-\frac{128}{9}S_{-5}$$
$$-\frac{8P_{22}}{9N^2(N+1)^2}S_{2,1}-\frac{128}{3}S_{2,3}+\frac{256}{9}S_{2,-3}-\frac{8(13N+4)(13N+9)}{27N(N+1)}S_{3,1}+\frac{256}{9}S_{4,1}$$
$$+\frac{64\big(10N^2+10N-3\big)}{27N(N+1)}S_{-2,2}-\frac{256}{9}S_{-2,3}-\frac{256}{9}S_{2,1,-2}+\frac{64}{3}S_{2,2,1}-\frac{256}{9}S_{3,1,1}$$
$$-\frac{256\big(10N^2+10N-3\big)}{27N(N+1)}S_{-2,1,1}-\frac{256}{9}S_{-2,2,1}+\frac{224}{9}S_{2,1,1,1}+\frac{1024}{9}S_{-2,1,1,1}\Big]$$
$$+C_FT_F^2\Big[-\frac{8\gamma_{qq}^{(0)}}{27}\left(2L_M^3+L_Q^3\right)+L_Q^2\Big[-\frac{8P_9}{27N^2(N+1)^2}+\frac{32}{9}S_1^2-\frac{32}{3}S_2$$
$$+\frac{16\big(29N^2+29N-6\big)}{27N(N+1)}S_1\Big]+L_M^2\Big[\frac{8P_4}{27N^2(N+1)^2}-\frac{320}{27}S_1+\frac{64}{9}S_2\Big]-L_M\frac{248\gamma_{qq}^{(0)}}{81}$$
$$+L_Q\Big[\frac{8P_{34}}{81N^3(N+1)^3}+\Big(-\frac{16P_{13}}{81N^2(N+1)^2}+\frac{64}{9}S_2\Big)S_1-\frac{16\big(29N^2+29N-6\big)}{27N(N+1)}S_1^2$$

$$
-\frac{64}{27}S_1^3+\frac{16\big(35N^2+35N-2\big)}{9N(N+1)}S_2-\frac{896}{27}S_3+\frac{128}{9}S_{2,1}\Bigg]-\frac{2P_{45}}{729N^4(N+1)^4}
$$
$$
+\frac{12064}{729}S_1+\frac{64}{81}S_2+\frac{320}{81}S_3-\frac{64}{27}S_4-\frac{112\gamma_{qq}^{(0)}\zeta_3}{27}\Bigg]
$$
$$
+C_FN_FT_F^2\Bigg[-\frac{8\gamma_{qq}^{(0)}}{27}\left(L_M^3+2L_Q^3\right)+L_Q^2\Bigg[-\frac{16P_9}{27N^2(N+1)^2}+\frac{64}{9}S_1^2-\frac{64}{3}S_2
$$
$$
+\frac{32\big(29N^2+29N-6\big)}{27N(N+1)}S_1\Bigg]+L_M\Bigg[\frac{4P_{33}}{81N^3(N+1)^3}-\frac{2176}{81}S_1-\frac{320}{27}S_2+\frac{64}{9}S_3\Bigg]
$$
$$
+L_Q\Bigg[\frac{16P_{34}}{81N^3(N+1)^3}+\left(-\frac{32P_{13}}{81N^2(N+1)^2}+\frac{128}{9}S_2\right)S_1-\frac{1792}{27}S_3
$$
$$
-\frac{32\big(29N^2+29N-6\big)}{27N(N+1)}S_1^2-\frac{128}{27}S_1^3+\frac{32\big(35N^2+35N-2\big)}{9N(N+1)}S_2+\frac{256}{9}S_{2,1}\Bigg]
$$
$$
+\frac{4P_{44}}{729N^4(N+1)^4}-\frac{24064}{729}S_1+\frac{128}{81}S_2+\frac{640}{81}S_3-\frac{128}{27}S_4+\frac{64\gamma_{qq}^{(0)}\zeta_3}{27}\Bigg]
$$
$$
+\frac{d^{abc}d^{abc}}{N_c}\frac{1}{2}L_Q\Bigg[-\frac{8P_{42}}{(N-1)N^5(N+1)^5(N+2)}+\frac{4P_{43}}{(N-1)N^4(N+1)^4(N+2)}S_1
$$
$$
+\frac{4\big(N^2+N+2\big)}{N^2(N+1)^2}S_3+\Bigg(\frac{16\big(N^2+N+2\big)^2}{(N-1)N^2(N+1)^2(N+2)}S_1
$$
$$
+\frac{8P_{27}}{(N-1)N^3(N+1)^3(N+2)}\Bigg)S_{-2}-\frac{8\big(N^2+N+2\big)}{N^2(N+1)^2}S_{-3}
$$
$$
+\frac{16\big(N^2+N+2\big)}{N^2(N+1)^2}S_{-2,1}\Bigg]+\hat{C}_{q,3}^{\rm NS,(3)}(N_F)\Bigg\}, \tag{2.11}
$$

where $\hat{C}_{q,3}^{\rm NS,(3)}(N_F)$ denotes the contribution due to the massless Wilson coefficient at 3-loop order [23], and the polynomials P_i are

$$
\begin{aligned}
P_1 &= -17N^4-34N^3-29N^2-12N-24 && (2.12)\\
P_2 &= -3N^4-6N^3-47N^2-20N+12 && (2.13)\\
P_3 &= N^4+2N^3-N^2-2N-4 && (2.14)\\
P_4 &= 3N^4+6N^3+47N^2+20N-12 && (2.15)\\
P_5 &= 7N^4+14N^3+3N^2-4N-4 && (2.16)\\
P_6 &= 19N^4+38N^3-9N^2-20N+4 && (2.17)\\
P_7 &= 28N^4+56N^3+28N^2+2N+1 && (2.18)\\
P_8 &= 33N^4+54N^3+9N^2-52N-28 && (2.19)\\
P_9 &= 57N^4+96N^3+65N^2-10N-24 && (2.20)\\
P_{10} &= 112N^4+224N^3+121N^2+9N+9 && (2.21)\\
P_{11} &= 141N^4+246N^3+241N^2-8N-84 && (2.22)\\
P_{12} &= 181N^4+266N^3+82N^2-3N+18 && (2.23)\\
P_{13} &= 235N^4+524N^3+211N^2+30N+72 && (2.24)\\
P_{14} &= 359N^4+772N^3+335N^2+30N+72 && (2.25)\\
P_{15} &= 501N^4+894N^3+541N^2-116N-204 && (2.26)
\end{aligned}
$$

$$P_{16} = 561N^4 + 1122N^3 + 767N^2 + 302N + 48 \quad (2.27)$$
$$P_{17} = 1131N^4 + 2118N^3 + 1307N^2 + 32N - 276 \quad (2.28)$$
$$P_{18} = 1139N^4 + 2710N^3 + 635N^2 + 216N + 828 \quad (2.29)$$
$$P_{19} = 1199N^4 + 2398N^3 + 1181N^2 + 18N + 90 \quad (2.30)$$
$$P_{20} = 1220N^4 + 2359N^3 + 1934N^2 + 357N - 138 \quad (2.31)$$
$$P_{21} = 3N^5 + 11N^4 + 10N^3 + 19N^2 + 23N + 16 \quad (2.32)$$
$$P_{22} = 12N^5 + 16N^4 + 18N^3 - 15N^2 - 5N - 8 \quad (2.33)$$
$$P_{23} = 27N^5 + 863N^4 + 1573N^3 + 1151N^2 + 144N - 36 \quad (2.34)$$
$$P_{24} = 648N^5 - 2103N^4 - 4278N^3 - 3505N^2 - 682N - 432 \quad (2.35)$$
$$P_{25} = -11145N^6 - 32355N^5 - 37523N^4 - 14329N^3 + 1240N^2 - 1032N - 2088 \quad (2.36)$$
$$P_{26} = -151N^6 - 469N^5 - 181N^4 + 305N^3 + 80N^2 - 88N - 56 \quad (2.37)$$
$$P_{27} = N^6 + 3N^5 - 8N^4 - 21N^3 - 23N^2 - 12N - 4 \quad (2.38)$$
$$P_{28} = 6N^6 + 18N^5 - N^4 - 20N^3 + 46N^2 + 29N - 6 \quad (2.39)$$
$$P_{29} = 15N^6 + 36N^5 + 30N^4 - 24N^3 + 3N^2 + 16N + 20 \quad (2.40)$$
$$P_{30} = 155N^6 + 465N^5 + 465N^4 + 155N^3 + 108N^2 + 108N + 54 \quad (2.41)$$
$$P_{31} = 216N^6 + 567N^5 + 687N^4 + 285N^3 + 37N^2 - 44N + 12 \quad (2.42)$$
$$P_{32} = 309N^6 + 807N^5 + 693N^4 - 463N^3 - 638N^2 + 68N + 216 \quad (2.43)$$
$$P_{33} = 525N^6 + 1575N^5 + 1535N^4 + 973N^3 + 536N^2 + 48N - 72 \quad (2.44)$$
$$P_{34} = 609N^6 + 1485N^5 + 1393N^4 + 83N^3 - 422N^2 + 156N + 216 \quad (2.45)$$
$$P_{35} = 795N^6 + 2043N^5 + 2075N^4 + 517N^3 - 298N^2 + 156N + 216 \quad (2.46)$$
$$P_{36} = 868N^6 + 2469N^5 + 2487N^4 + 940N^3 + 171N^2 + 207N + 144 \quad (2.47)$$
$$P_{37} = 1407N^6 + 3825N^5 + 4211N^4 + 1783N^3 - 250N^2 - 240N + 144 \quad (2.48)$$
$$P_{38} = 1770N^6 + 4671N^5 + 4765N^4 + 1205N^3 - 227N^2 + 1044N + 756 \quad (2.49)$$
$$P_{39} = 7531N^6 + 23673N^5 + 23055N^4 + 7375N^3 + 1614N^2 + 936N - 324 \quad (2.50)$$
$$P_{40} = -4785N^8 - 19140N^7 - 18754N^6 + 1320N^5 + 12723N^4 + 6548N^3 + 4080N^2 - 648N - 1728 \quad (2.51)$$
$$P_{41} = -45N^8 - 162N^7 - 858N^6 - 936N^5 - 1629N^4 - 1094N^3 - 804N^2 - 40N + 192 \quad (2.52)$$
$$P_{42} = N^8 + 4N^7 + 13N^6 + 25N^5 + 57N^4 + 77N^3 + 55N^2 + 20N + 4 \quad (2.53)$$
$$P_{43} = 3N^8 + 12N^7 + 16N^6 + 6N^5 + 30N^4 + 64N^3 + 73N^2 + 40N + 12 \quad (2.54)$$
$$P_{44} = 3549N^8 + 14196N^7 + 23870N^6 + 25380N^5 + 15165N^4 + 1712N^3 - 2016N^2 + 144N + 432 \quad (2.55)$$
$$P_{45} = 5487N^8 + 21948N^7 + 36370N^6 + 28836N^5 + 11943N^4 + 4312N^3 + 2016N^2 - 144N - 432 \quad (2.56)$$
$$P_{46} = 10807N^8 + 43228N^7 + 63222N^6 + 40150N^5 + 14587N^4 + 9018N^3 + 7452N^2 + 2376N + 324 \quad (2.57)$$
$$P_{47} = 42591N^8 + 166764N^7 + 245664N^6 + 129982N^5 - 13295N^4 - 25978N^3 + 3560N^2 - 3192N - 4464 \quad (2.58)$$
$$P_{48} = -18351N^{10} - 89784N^9 - 210021N^8 - 271638N^7 - 219369N^6 - 90572N^5 - 26491N^4 - 7790N^3 - 1992N^2 - 2760N - 2160 \quad (2.59)$$

$$
\begin{aligned}
P_{49} &= 165N^{10} + 825N^9 + 109664N^8 + 331682N^7 + 457641N^6 + 346145N^5 \\
&\quad +219290N^4 + 86724N^3 + 13608N^2 + 14256N + 10368 \qquad (2.60)\\
P_{50} &= 828N^{10} + 3492N^9 + 4305N^8 - 2013N^7 - 8540N^6 - 3822N^5 - 1157N^4 \\
&\quad -3057N^3 - 4112N^2 - 324N + 576 \qquad (2.61)\\
P_{51} &= 8274N^{10} + 37149N^9 + 53630N^8 + 7538N^7 - 59902N^6 - 55159N^5 \\
&\quad -6994N^4 + 3272N^3 - 9048N^2 - 1656N + 2160 \; . \qquad (2.62)
\end{aligned}
$$

Here $C_A = N_c, C_F = (N_c^2-1)/(2N_c), T_F = 1/2$ and $d^{abc}d^{abc}/N_c = (N_c^2-1)(N_c^2-4)/N_c^2$ denote the color factors for $SU(N_c)$, with $N_c = 3$ in case of QCD. The constant B_4 is given by

$$
B_4 = -4\zeta_2 \ln^2(2) + \frac{2}{3}\ln^4(2) - \frac{13}{2}\zeta_4 + 16\mathrm{Li}_4\left(\frac{1}{2}\right), \qquad (2.63)
$$

which is related to multiple zeta values [41], $\zeta_n = \sum_{k=1}^{\infty} 1/k^n, \;\; n \in \mathbb{N}, n \geq 2$, denote the values of Riemann's ζ-function at integer argument and $\mathrm{Li}_n(x), n \in \mathbb{N}$, is the polylogarithm [42]. Terms containing the color factor $d^{abc}d^{abc}/N_c$ stem only from the massless Wilson coefficient and the non-singlet valence anomalous dimension at 3-loop order [43], cf. Appendix A.

One obtains the analytic continuation of the harmonic sums to complex values of N by performing their asymptotic expansion analytically, cf. [44,45]. These expansions can be obtained automatically using the package `HarmonicSums` [39]. Furthermore, the nested harmonic sums obey the shift relations

$$
S_{b,\vec{a}}(N) = S_{b,\vec{a}}(N-1) + \frac{(\mathrm{sign}(b))^N}{N^{|b|}} S_{\vec{a}}(N) \; , \qquad (2.64)
$$

through which any regular point in the complex plane can be reached using the analytic asymptotic representation as input. The poles of the nested harmonic sums $S_{\vec{a}}(N)$ are located at the non-positive integers. In data analyses, one may thus encode the QCD evolution [5] together with the Wilson coefficient for complex values of N analytically and finally perform one numerical contour integral around the singularities of the problem.[5]

In x-space the Wilson coefficient is represented in terms of harmonic polylogarithms [47] over the alphabet $\{f_0, f_1, f_{-1}\}$, which were again reduced applying the shuffle relations [48]. They are defined by

$$
\begin{aligned}
H_{b,\vec{a}}(x) &= \int_0^x dy f_b(y) H_{\vec{a}}(y), \quad H_{\underbrace{0,...,0}_{k}}(x) = \frac{1}{k!}\ln^k(x), \quad H_{\emptyset} = 1, \qquad (2.65)\\
f_0(x) &= \frac{1}{x}, \qquad f_1(x) = \frac{1}{1-x}, \qquad f_{-1}(x) = \frac{1}{1+x} \; . \qquad (2.66)
\end{aligned}
$$

The Wilson coefficient is represented by three contributions, the $(...)_+$-distribution, the $\delta(1-x)$-term, and the regular term, with the +-distribution being defined by

$$
\int_0^1 dy \left[F(y)\right]_+ g(y) = \int_0^1 dy F(y) \left[g(y) - g(1)\right] \; . \qquad (2.67)
$$

It reads

[5] For precise numerical implementations of the analytic continuation of harmonic sums see [46].

$$
\begin{aligned}
&L_{q,3}^{W^+-W^-,\mathrm{NS}}(x) = \\
&a_s^2\Bigg\{\Bigg(\frac{1}{1-x}C_F T_F\Bigg[L_M^2\frac{8}{3}+L_Q^2\frac{8}{3}+L_M\Bigg[\frac{80}{9}+\frac{16}{3}H_0\Bigg]+L_Q\Bigg[-\frac{116}{9}-\frac{32}{3}H_0-\frac{16}{3}H_1\Bigg] \\
&+\frac{718}{27}-\frac{32}{3}\zeta_2+\frac{268}{9}H_0+8H_0^2+\Bigg(\frac{116}{9}+\frac{16}{3}H_0\Bigg)H_1+\frac{8}{3}H_1^2+\frac{16}{3}H_{0,1}\Bigg]\Bigg)_+ \\
&+\delta(1-x)\Bigg(C_F T_F\Bigg[L_M^2 2+L_Q^2 2+L_M\frac{2}{3}-L_Q\frac{38}{3}+\frac{265}{9}\Bigg]\Bigg) \\
&+C_F T_F\Bigg[-\left(L_M^2+L_Q^2\right)\frac{4}{3}(x+1)+L_M\Bigg[-\frac{8}{9}(11x-1)-\frac{8}{3}(x+1)H_0\Bigg] \\
&+L_Q\Bigg[\frac{8}{9}(14x+5)+\frac{16}{3}(x+1)H_0+\frac{8}{3}(x+1)H_1\Bigg]-\frac{4}{27}(218x+47)+\frac{16}{3}(x+1)\zeta_2 \\
&-\frac{8}{9}(28x+13)H_0-4(x+1)H_0^2+\Bigg(-\frac{8}{9}(14x+5)-\frac{8}{3}(x+1)H_0\Bigg)H_1 \\
&-\frac{4}{3}(x+1)H_1^2-\frac{8}{3}(x+1)H_{0,1}\Bigg]\Bigg\} \\
&+a_s^3\Bigg\{\Bigg(\frac{1}{(1-x)^2}C_A C_F T_F\Bigg[\frac{32}{81}(94x-121)\zeta_2-\frac{4}{81}(800x-773)H_0^2 \\
&+\frac{32}{9}(x+2)H_{0,1}\Bigg]+\frac{1}{1-x}\Bigg(C_A C_F T_F\Bigg[-L_M^3\frac{176}{27}-L_Q^3\frac{352}{27}+L_M^2\Bigg[\frac{184}{9}-\frac{32}{3}\zeta_2 \\
&+\frac{16}{3}H_0^2\Bigg]+L_Q^2\Bigg[\frac{3104}{27}-\frac{32}{3}\zeta_2+\frac{704}{9}H_0+\frac{16}{3}H_0^2+\frac{352}{9}H_1\Bigg]+L_M\Bigg[\frac{1240}{81}+\Bigg(-\frac{320}{9} \\
&-\frac{64}{3}H_0\Bigg)\zeta_2+96\zeta_3+\frac{1792}{27}H_0+\frac{248}{9}H_0^2+\frac{32}{9}H_0^3-16H_0^2H_1+32H_0H_{0,1}-\frac{64}{3}H_{0,0,1}\Bigg] \\
&+L_Q\Bigg[-\frac{30124}{81}+\Bigg(192+\frac{128}{3}H_0+64H_1\Bigg)\zeta_2-\frac{256}{3}\zeta_3-\frac{14144}{27}H_0-\frac{1216}{9}H_0^2 \\
&-\frac{80}{9}H_0^3+\Bigg(-\frac{6208}{27}-\frac{704}{9}H_0-\frac{16}{3}H_0^2\Bigg)H_1+\Bigg(-\frac{352}{9}+\frac{32}{3}H_0\Bigg)H_1^2-64H_0H_{0,-1} \\
&+\Bigg(-\frac{704}{9}+\frac{32}{3}H_0-\frac{128}{3}H_1\Bigg)H_{0,1}+128H_{0,0,-1}-\frac{128}{3}H_{0,0,1}+64H_{0,1,1}\Bigg]+\frac{43228}{729} \\
&-\frac{32}{3}B_4+\Bigg(-\frac{496}{27}H_0-\frac{112}{9}H_0^2+\Bigg(8-\frac{160}{9}H_0\Bigg)H_1-\frac{128}{9}H_1^2+\frac{32}{9}H_{0,1}\Bigg)\zeta_2 \\
&+\Bigg(-\frac{1196}{27}+\frac{160}{9}H_0-\frac{32}{9}H_1\Bigg)\zeta_3+\frac{296}{3}\zeta_4+\frac{3256}{81}H_0+\frac{496}{81}H_0^3+\frac{16}{27}H_0^4 \\
&+\Bigg(-\frac{32}{3}(x-2)-\frac{32}{9}H_0-\frac{160}{9}H_0^2-\frac{112}{27}H_0^3\Bigg)H_1+\frac{8}{9}H_0^2H_1^2-\frac{64}{27}H_0H_1^3 \\
&+\Bigg(\frac{368}{9}H_0+\frac{16}{3}H_0^2+\Bigg(-8-\frac{128}{9}H_0\Bigg)H_1+\frac{128}{9}H_1^2\Bigg)H_{0,1}-\frac{32}{9}H_{0,1}^2+\Bigg(-\frac{1072}{27}
\end{aligned}
$$

$$+\frac{32}{9}H_0+\frac{320}{9}H_1\Big)H_{0,0,1}+\Big(24+\frac{160}{9}H_0-32H_1\Big)H_{0,1,1}-\frac{224}{9}\left(H_{0,0,1,1}-H_{0,1,1,1}\right)\Big]$$
$$+C_F^2T_F\Big[L_Q^3\Big[16-\frac{32}{3}H_0-\frac{64}{3}H_1\Big]+L_M^2L_Q\Big[16-\frac{32}{3}H_0-\frac{64}{3}H_1\Big]+L_Q^2\Big[-\frac{334}{3}$$
$$-\frac{256}{3}\zeta_2+\frac{32}{9}H_0+\frac{80}{3}H_0^2+\Big(\frac{856}{9}+\frac{320}{3}H_0\Big)H_1+48H_1^2\Big]+L_M^2\Big[-22-\frac{64}{3}\zeta_2$$
$$-16H_0+\frac{16}{3}H_0^2+\Big(8+\frac{128}{3}H_0\Big)H_1+16H_1^2\Big]+L_ML_Q\Big[\frac{88}{3}+\frac{64}{3}\zeta_2-\frac{176}{9}H_0$$
$$-\frac{32}{3}H_0^2+\Big(-\frac{640}{9}-\frac{64}{3}H_0\Big)H_1\Big]+L_M\Big[-\frac{206}{3}+\Big(-\frac{784}{9}-\frac{128}{3}H_0-\frac{64}{3}H_1\Big)\zeta_2$$
$$-64\zeta_3-\frac{112}{3}H_0+\frac{88}{9}H_0^2+\frac{64}{9}H_0^3+\Big(\frac{152}{3}+\frac{1424}{9}H_0+\frac{160}{3}H_0^2\Big)H_1+\Big(\frac{160}{3}$$
$$+\frac{32}{3}H_0\Big)H_1^2-\frac{64}{3}H_0H_{0,1}\Big]+L_Q\Big[\frac{2360}{9}+\Big(\frac{2608}{9}+\frac{832}{3}H_0+\frac{448}{3}H_1\Big)\zeta_2+320\zeta_3$$
$$+\frac{4508}{27}H_0-\frac{160}{3}H_0^2-\frac{224}{9}H_0^3+\Big(-\frac{4556}{27}-\frac{3680}{9}H_0-128H_0^2\Big)H_1+\Big(-\frac{512}{3}$$
$$-128H_0\Big)H_1^2-\frac{320}{9}H_1^3+128H_0H_{0,-1}+\Big(48-\frac{64}{3}H_0+\frac{64}{3}H_1\Big)H_{0,1}-256H_{0,0,-1}$$
$$-64H_{0,1,1}\Big]-\frac{14197}{54}+\frac{64}{3}B_4+\Big(-\frac{2488}{27}-\frac{1192}{27}H_0-\frac{80}{9}H_0^2+\Big(-\frac{160}{9}+\frac{32}{3}H_0\Big)H_1$$
$$+\frac{128}{9}H_1^2-\frac{32}{9}H_{0,1}\Big)\zeta_2+\Big(\frac{3088}{27}-\frac{128}{9}H_0+\frac{160}{9}H_1\Big)\zeta_3-\frac{664}{9}\zeta_4-\frac{3262}{27}H_0$$
$$+\frac{196}{27}H_0^2+\frac{380}{81}H_0^3+\frac{4}{3}H_0^4+\Big(\frac{302}{9}+\frac{13624}{81}H_0+\frac{1628}{27}H_0^2+\frac{304}{27}H_0^3\Big)H_1$$
$$+\Big(\frac{448}{9}+\frac{80}{9}H_0-\frac{8}{9}H_0^2\Big)H_1^2+\frac{128}{27}H_0H_1^3+\Big(\frac{112}{9}-\frac{1304}{27}H_0-\frac{32}{3}H_0^2+\frac{160}{9}H_0H_1$$
$$-\frac{128}{9}H_1^2\Big)H_{0,1}-\frac{16}{9}H_{0,1}^2+\Big(\frac{1184}{27}+\frac{128}{9}H_0-\frac{256}{9}H_1\Big)H_{0,0,1}+\Big(-16-\frac{32}{3}H_0$$
$$+\frac{64}{3}H_1\Big)H_{0,1,1}-\frac{128}{9}H_{0,0,0,1}+\frac{64}{3}H_{0,0,1,1}\Big]+C_FT_F^2\Big[L_M^3\frac{128}{27}+L_Q^3\frac{64}{27}+L_M^2\Big[\frac{320}{27}$$
$$+\frac{64}{9}H_0\Big]+L_Q^2\Big[-\frac{464}{27}-\frac{128}{9}H_0-\frac{64}{9}H_1\Big]+L_M\frac{1984}{81}+L_Q\Big[\frac{3760}{81}-\frac{256}{9}\zeta_2$$
$$+\frac{2144}{27}H_0+\frac{64}{3}H_0^2+\Big(\frac{928}{27}+\frac{128}{9}H_0\Big)H_1+\frac{64}{9}H_1^2+\frac{128}{9}H_{0,1}\Big]-\frac{12064}{729}+\frac{896}{27}\zeta_3$$
$$+\frac{64}{81}H_0-\frac{160}{81}H_0^2-\frac{32}{81}H_0^3\Big]+C_FN_FT_F^2\Big[L_M^3\frac{64}{27}+L_Q^3\frac{128}{27}+L_Q^2\Big[-\frac{928}{27}-\frac{256}{9}H_0$$
$$-\frac{128}{9}H_1\Big]+L_M\Big[\frac{2176}{81}-\frac{320}{27}H_0-\frac{32}{9}H_0^2\Big]+L_Q\Big[\frac{7520}{81}-\frac{512}{9}\zeta_2+\frac{4288}{27}H_0$$
$$+\frac{128}{3}H_0^2+\Big(\frac{1856}{27}+\frac{256}{9}H_0\Big)H_1+\frac{128}{9}H_1^2+\frac{256}{9}H_{0,1}\Big]+\frac{24064}{729}-\frac{512}{27}\zeta_3+\frac{128}{81}H_0$$

$$-\frac{320}{81}H_0^2-\frac{64}{81}H_0^3\Bigg]\Bigg)\Bigg)_+ + \delta(1-x)\Bigg(C_AC_FT_F\Bigg[-L_M^3\frac{44}{9}-L_Q^3\frac{88}{9}+L_M^2\Bigg[\frac{34}{3}-\frac{16}{3}\zeta_3\Bigg]$$
$$+L_Q^2\Bigg[\frac{938}{9}-\frac{16}{3}\zeta_3\Bigg]+L_M\Bigg[-\frac{1595}{27}+\frac{272}{9}\zeta_3+\frac{68}{3}\zeta_4\Bigg]+L_Q\Bigg[-\frac{11032}{27}-\frac{32}{3}\zeta_2$$
$$+\frac{1024}{9}\zeta_3-\frac{196}{3}\zeta_4\Bigg]+\frac{2647}{243}-8B_4-\frac{10045}{81}\zeta_3-\frac{16}{9}\zeta_2\zeta_3+\frac{2624}{27}\zeta_4-\frac{176}{9}\zeta_5\Bigg]$$
$$+C_F^2T_F\Bigg[6L_Q\left(L_Q^2+L_M^2\right)+L_M^2\Bigg[-10+\frac{32}{3}\zeta_3\Bigg]+L_Q^2\Bigg[-48+\frac{32}{3}\zeta_3\Bigg]+2L_ML_Q$$
$$+L_M\Bigg[-5-\frac{112}{9}\zeta_3-\frac{136}{3}\zeta_4\Bigg]+L_Q\Bigg[\frac{368}{3}+\frac{64}{3}\zeta_2-\frac{1616}{9}\zeta_3+\frac{392}{3}\zeta_4\Bigg]-\frac{2039}{18}$$
$$+16B_4+\frac{13682}{81}\zeta_3+\frac{32}{9}\zeta_2\zeta_3-\frac{3304}{27}\zeta_4+\frac{352}{9}\zeta_5\Bigg]+C_FT_F^2\Bigg[L_M^3\frac{32}{9}+L_Q^3\frac{16}{9}+L_M^2\frac{8}{9}$$
$$-L_Q^2\frac{152}{9}+L_M\frac{496}{27}+L_Q\frac{1624}{27}-\frac{3658}{243}+\frac{224}{9}\zeta_3\Bigg]+C_FN_FT_F^2\Bigg[L_M^3\frac{16}{9}+L_Q^3\frac{32}{9}$$
$$-L_Q^2\frac{304}{9}+L_M\frac{700}{27}+L_Q\frac{3248}{27}+\frac{4732}{243}-\frac{128}{9}\zeta_3\Bigg]\Bigg)+C_AC_FT_F\Bigg[L_M^3\frac{88}{27}(x+1)$$
$$+L_Q^3\frac{176}{27}(x+1)+L_M^2\Bigg[-\frac{4}{9}(83x-37)+\frac{32}{3}\frac{x}{x+1}\zeta_2+\frac{32}{3}(x+1)H_0$$
$$-\frac{32}{3}\frac{x^2+1}{x+1}H_{-1}H_0-\frac{16}{3}\frac{x}{x+1}H_0^2+\frac{32}{3}\frac{x^2+1}{x+1}H_{0,-1}\Bigg]+L_Q^2\Bigg[-\frac{4}{27}(865x+109)$$
$$+\frac{32}{3}\frac{x}{x+1}\zeta_2-\frac{256}{9}(x+1)H_0-\frac{32}{3}\frac{x^2+1}{x+1}H_{-1}H_0-\frac{16}{3}\frac{x}{x+1}H_0^2-\frac{176}{9}(x+1)H_1$$
$$+\frac{32}{3}\frac{x^2+1}{x+1}H_{0,-1}\Bigg]+L_M\Bigg[-\frac{4}{81}(4577x-4267)+\Bigg(\frac{16}{9}\frac{3x^2+14x-9}{x+1}$$
$$-\frac{64}{3}\frac{x^2+1}{x+1}H_{-1}+\frac{16}{3}\frac{3x^2+4x+3}{x+1}H_0\Bigg)\zeta_2-32\frac{x^2+3x+1}{x+1}\zeta_3-\frac{16}{27}(29x-109)H_0$$
$$+\frac{4}{9}\frac{19x^2+4x+25}{x+1}H_0^2-\frac{32}{9}\frac{x}{x+1}H_0^3+\Bigg(\frac{32}{3}(x-1)+8(x+1)H_0^2\Bigg)H_1$$
$$+\frac{128}{9}\frac{4x^2+3x+4}{x+1}H_{0,-1}+\Bigg(-\frac{16}{3}(x+1)-16(x+1)H_0\Bigg)H_{0,1}$$
$$+\Bigg(-\frac{128}{9}\frac{4x^2+3x+4}{x+1}H_0-\frac{16}{3}\frac{x^2+1}{x+1}H_0^2+\frac{64}{3}\frac{x^2+1}{x+1}H_{0,1}\Bigg)H_{-1}-\frac{64}{3}\frac{x^2+1}{x+1}H_{0,-1,1}$$
$$+\frac{32}{3}\frac{x^2+1}{x+1}H_{0,0,-1}+\frac{64}{3}\frac{x}{x+1}H_{0,0,1}-\frac{64}{3}\frac{x^2+1}{x+1}H_{0,1,-1}\Bigg]+L_Q\Bigg[\frac{4}{81}(12329x-577)$$
$$+\Bigg(\frac{16}{9}\frac{12x^3-23x^2-72x-17}{x+1}-\frac{32}{3}\frac{(x-1)^2}{x+1}H_{-1}-\frac{16}{3}\frac{3x^2+8x+3}{x+1}H_0$$
$$-\frac{64}{3}(x+2)H_1\Bigg)\zeta_2+\frac{64}{3}\frac{3x^2+3x+2}{x+1}\zeta_3+\Bigg(\frac{64}{27}\frac{181x^2+239x+49}{x+1}$$
$$+\frac{32}{9}\frac{6x^4+25x^3+18x^2+25x+6}{(x+1)x}H_{-1}-\frac{32}{3}\frac{(x-1)^2}{x+1}H_{-1}^2\Bigg)H_0$$

$$
+\left(-\frac{8}{9}\frac{12x^3-21x^2-77x-24}{x+1}+\frac{16}{3}\frac{5x^2-2x+5}{x+1}H_{-1}\right)H_0^2+\frac{80}{9}\frac{x}{x+1}H_0^3
$$
$$
+\left(\frac{8}{27}\big(703x+253\big)+\frac{352}{9}\big(x+1\big)H_0-\frac{8}{3}\big(x-3\big)H_0^2\right)H_1+\left(\frac{176}{9}\big(x+1\big)\right.
$$
$$
\left.-\frac{16}{3}\big(x+1\big)H_0\right)H_1^2+\left(-\frac{32}{9}\frac{6x^4+25x^3+18x^2+25x+6}{\big(x+1\big)x}+\frac{64}{3}\frac{\big(x-1\big)^2}{x+1}H_{-1}\right.
$$
$$
\left.+\frac{64}{3}\frac{3x+1}{x+1}H_0\right)H_{0,-1}+\left(\frac{208}{9}\big(x+1\big)+\frac{16}{3}\big(x-3\big)H_0+\frac{64}{3}\big(x+1\big)H_1\right)H_{0,1}
$$
$$
-\frac{64}{3}\frac{\big(x-1\big)^2}{x+1}H_{0,-1,-1}-\frac{32}{3}\frac{5x^2+10x+9}{x+1}H_{0,0,-1}+\frac{32}{3}\big(x+3\big)H_{0,0,1}
$$
$$
\left.-32\big(x+1\big)H_{0,1,1}\right]-\frac{2}{729}\big(108295x-86681\big)+\frac{16}{3}\big(x+1\big)B_4
$$
$$
+\left(\frac{16}{81}\frac{174x^2+209x-189}{x+1}-\frac{32}{27}\frac{29x^2+18x+29}{x+1}H_{-1}-\frac{32}{9}\frac{x^2+1}{x+1}H_{-1}^2\right.
$$
$$
\left.+\left(\frac{8}{27}\frac{63x^2+29x+6}{x+1}-\frac{32}{9}\frac{x^2+1}{x+1}H_{-1}\right)H_0+\frac{8}{9}\frac{3x^2+8x+9}{x+1}H_0^2\right.
$$
$$
\left.+\left(-\frac{8}{9}\big(3x+14\big)+\frac{80}{9}\big(x+1\big)H_0\right)H_1+\frac{64}{9}\big(x+1\big)H_1^2-\frac{16}{9}\big(7x+1\big)H_{0,1}\right)\zeta_2
$$
$$
+\left(\frac{2}{27}\frac{497x^2+1102x+1085}{x+1}+\frac{128}{9}\frac{x^2+1}{x+1}H_{-1}+\frac{32}{9}\frac{6x^2+4x-3}{x+1}H_0\right.
$$
$$
\left.+\frac{16}{9}\big(x+1\big)H_1\right)\zeta_3-\frac{8}{3}\frac{36x^2+51x+22}{x+1}\zeta_4+\left(-\frac{4}{81}\big(995x-2807\big)\right.
$$
$$
\left.-\frac{32}{81}\frac{199x^2+174x+199}{x+1}H_{-1}+\frac{32}{9}\big(x+1\big)H_{-1}^2-\frac{64}{27}\frac{x^2+1}{x+1}H_{-1}^3\right)H_0
$$
$$
+\left(\frac{4}{81}\frac{253x^2+391x+586}{x+1}-\frac{16}{27}\frac{19x^2+18x+19}{x+1}H_{-1}+\frac{16}{9}\frac{x^2+1}{x+1}H_{-1}^2\right)H_0^2
$$
$$
+\left(\frac{8}{81}\frac{22x^2+7x+25}{x+1}-\frac{32}{27}\frac{x^2+1}{x+1}H_{-1}\right)H_0^3-\frac{16}{27}\frac{x}{x+1}H_0^4+\left(-\frac{8}{27}\big(65x+7\big)\right.
$$
$$
\left.+\frac{8}{9}\big(9x+4\big)H_0+\frac{8}{9}\big(14x+3\big)H_0^2+\frac{56}{27}\big(x+1\big)H_0^3\right)H_1+\left(-\frac{4}{9}\big(43x-46\big)\right.
$$
$$
\left.-\frac{8}{9}\big(2x+5\big)H_0-\frac{4}{9}\big(x+1\big)H_0^2\right)H_1^2+\frac{32}{27}\big(x+1\big)H_0H_1^3+\left(-\frac{64}{9}\big(x+1\big)H_{-1}\right.
$$
$$
\left.+\frac{32}{81}\frac{199x^2+174x+199}{x+1}+\frac{64}{9}\frac{x^2+1}{x+1}H_{-1}^2\right)H_{0,-1}+\left(-\frac{8}{27}\big(143x+2\big)\right.
$$
$$
+\frac{256}{27}\frac{4x^2+3x+4}{x+1}H_{-1}-\frac{16}{9}\big(13x+6\big)H_0-\frac{8}{3}\big(x+1\big)H_0^2+\left(\frac{8}{9}\big(11x+20\big)\right.
$$
$$
\left.+\frac{64}{9}\big(x+1\big)H_0\right)H_1-\frac{64}{9}\big(x+1\big)H_1^2\Big)H_{0,1}+\frac{16}{9}\big(7x+1\big)H_{0,1}^2+\left(\frac{64}{9}\big(x+1\big)\right.
$$
$$
\left.-\frac{128}{9}\frac{x^2+1}{x+1}H_{-1}\right)H_{0,-1,-1}-\frac{256}{27}\frac{4x^2+3x+4}{x+1}H_{0,-1,1}+\left(\frac{32}{27}\frac{19x^2+18x+19}{x+1}\right.
$$
$$
\left.-\frac{64}{9}\frac{x^2+1}{x+1}H_{-1}\right)H_{0,0,-1}+\left(\frac{8}{27}\frac{9x^2+101x+12}{x+1}+\frac{64}{9}\frac{x^2+1}{x+1}H_{-1}-\frac{16}{9}\big(7x+1\big)H_0\right.
$$

$$
-\frac{160}{9}(x+1)H_1\Big)H_{0,0,1} - \frac{256}{27}\frac{4x^2+3x+4}{x+1}H_{0,1,-1} + \Big(16(x+1)H_1 - \frac{16}{9}(x+7)
$$
$$
-\frac{128}{9}\frac{x^2+1}{x+1}H_{-1} - \frac{16}{9}(11x+5)H_0\Big)H_{0,1,1} + \frac{128}{9}\frac{x^2+1}{x+1}\big(H_{0,-1,-1,-1} + H_{0,-1,1,1}
$$
$$
+\frac{1}{2}\big(H_{0,0,-1,-1} - H_{0,0,-1,1} + H_{0,0,0,-1} - H_{0,0,1,-1}\big) + H_{0,1,-1,1} + H_{0,1,1,-1}\big)
$$
$$
+\frac{64}{9}\frac{5x^2+6x-1}{x+1}H_{0,0,0,1} - \frac{16}{9}\frac{x^2-2x-11}{x+1}H_{0,0,1,1} - \frac{112}{9}(x+1)H_{0,1,1,1}\Big]
$$
$$
+C_F^2T_F\Big[L_Q^3\Big[-\frac{8}{3}(x+5) + 8(x+1)H_0 + \frac{32}{3}(x+1)H_1\Big] + L_M^2L_Q\Big[-\frac{8}{3}(x+5)
$$
$$
+8(x+1)H_0 + \frac{32}{3}(x+1)H_1\Big] + L_M^2\Big[28(2x-1) + \frac{8}{3}\frac{9x^2+10x+9}{x+1}\zeta_2
$$
$$
+\Big(-\frac{8}{3}(11x+5) + \frac{64}{3}\frac{x^2+1}{x+1}H_{-1}\Big)H_0 - \frac{4}{3}\frac{9x^2+10x+9}{x+1}H_0^2 + \Big(-\frac{16}{3}(2x+1)
$$
$$
-\frac{64}{3}(x+1)H_0\Big)H_1 - 8(x+1)H_1^2 - \frac{64}{3}\frac{x^2+1}{x+1}H_{0,-1} - \frac{8}{3}(x+1)H_{0,1}\Big]
$$
$$
+L_Q^2\Big[\frac{4}{9}(161x+130) + \frac{8}{3}\frac{23x^2+38x+23}{x+1}\zeta_2 + \Big(\frac{64}{3}\frac{x^2+1}{x+1}H_{-1} - \frac{16}{3}(15x+4)\Big)H_0
$$
$$
-\frac{4}{3}\frac{21x^2+34x+21}{x+1}H_0^2 + \Big(-\frac{16}{9}(50x+17) - \frac{160}{3}(x+1)H_0\Big)H_1 - 24(x+1)H_1^2
$$
$$
-\frac{64}{3}\frac{x^2+1}{x+1}H_{0,-1} - 8(x+1)H_{0,1}\Big] + L_ML_Q\Big[\frac{4}{9}(19x-85) - \frac{32}{3}(x+1)\zeta_2
$$
$$
+\frac{8}{3}(13x+1)H_0 + 8(x+1)H_0^2 + \Big(\frac{128}{9}(4x+1) + \frac{32}{3}(x+1)H_0\Big)H_1\Big]
$$
$$
+L_M\Big[\frac{4}{3}(178x-125) + \Big(\frac{8}{9}\frac{117x^2+118x+81}{x+1} + \frac{128}{3}\frac{x^2+1}{x+1}H_{-1}
$$
$$
+\frac{16}{3}\frac{(x+3)(3x+1)}{x+1}H_0 + \frac{32}{3}(x+1)H_1\Big)\zeta_2 - \frac{4}{9}\frac{195x^2+238x+123}{x+1}H_0^2
$$
$$
+\frac{16}{3}\frac{x^2+14x+1}{x+1}\zeta_3 - \frac{4}{9}(337x+235)H_0 - \frac{32}{9}\frac{3x^2+4x+3}{x+1}H_0^3 + \Big(-\frac{4}{9}(287x-113)
$$
$$
-\frac{224}{9}(5x+2)H_0 - \frac{80}{3}(x+1)H_0^2\Big)H_1 - \Big(\frac{16}{3}(7x+3) + \frac{16}{3}(x+1)H_0\Big)H_1^2
$$
$$
-\frac{256}{9}\frac{4x^2+3x+4}{x+1}H_{0,-1} + \Big(\frac{184}{9}(x+1) + \frac{32}{3}(x+1)H_0\Big)H_{0,1}
$$
$$
+\Big(\frac{256}{9}\frac{4x^2+3x+4}{x+1}H_0 + \frac{32}{3}\frac{x^2+1}{x+1}H_0^2 - \frac{128}{3}\frac{x^2+1}{x+1}H_{0,1}\Big)H_{-1}
$$
$$
+\frac{64}{3}\frac{x^2+1}{x+1}\left(2H_{0,-1,1} - H_{0,0,-1} + 2H_{0,1,-1}\right) + \frac{16}{3}\frac{3x^2-2x+3}{x+1}H_{0,0,1}\Big]
$$
$$
+L_Q\Big[-\frac{8}{27}(557x+652) + \Big(-\frac{16}{9}\frac{24x^3+245x^2+318x+137}{x+1} + \frac{64}{3}\frac{(x-1)^2}{x+1}H_{-1}
$$
$$
-\frac{16}{3}\frac{35x^2+66x+35}{x+1}H_0 - \frac{32}{3}(9x+5)H_1\Big)\zeta_2 - \frac{32}{3}\frac{21x^2+30x+17}{x+1}\zeta_3
$$

$$
+\Bigg(\frac{8}{9}\frac{115x^2+99x+32}{x+1}-\frac{64}{9}\frac{6x^4+25x^3+18x^2+25x+6}{(x+1)x}H_{-1}
$$
$$
+\frac{64}{3}\frac{(x-1)^2}{x+1}H_{-1}^2\Bigg)H_0+\Bigg(\frac{4}{9}\frac{48x^3+519x^2+706x+315}{x+1}-\frac{32}{3}\frac{5x^2-2x+5}{x+1}H_{-1}\Bigg)H_0^2
$$
$$
+\frac{32}{9}\frac{9x^2+13x+9}{x+1}H_0^3+\Bigg(\frac{8}{27}\big(908x-19\big)+\frac{16}{9}\big(169x+97\big)H_0+\frac{32}{3}\big(7x+5\big)H_0^2\Bigg)H_1
$$
$$
+\Bigg(\frac{32}{3}\big(13x+6\big)+64\big(x+1\big)H_0\Bigg)H_1^2+\frac{160}{9}\big(x+1\big)H_1^3+\Bigg(-\frac{128}{3}\frac{(x-1)^2}{x+1}H_{-1}
$$
$$
+\frac{64}{9}\frac{6x^4+25x^3+18x^2+25x+6}{(x+1)x}-\frac{128}{3}\frac{3x+1}{x+1}H_0\Bigg)H_{0,-1}+\Bigg(\frac{64}{9}\big(13x+1\big)
$$
$$
+\frac{16}{3}\big(x+9\big)H_0-\frac{32}{3}\big(x+1\big)H_1\Bigg)H_{0,1}+\frac{128}{3}\frac{(x-1)^2}{x+1}H_{0,-1,-1}+\frac{16}{3}\big(5x-3\big)H_{0,0,1}
$$
$$
+48\big(x+1\big)H_{0,1,1}+\frac{64}{3}\frac{5x^2+10x+9}{x+1}H_{0,0,-1}\Bigg]+\frac{1}{27}\big(12332x-4905\big)-\frac{32}{3}\big(x+1\big)B_4
$$
$$
+\Bigg(\frac{4}{81}\frac{1619x^2+1338x+1511}{x+1}+\frac{64}{27}\frac{29x^2+18x+29}{x+1}H_{-1}+\frac{64}{9}\frac{x^2+1}{x+1}H_{-1}^2
$$
$$
+\Bigg(\frac{4}{27}\frac{147x^2+298x-9}{x+1}+\frac{64}{9}\frac{x^2+1}{x+1}H_{-1}\Bigg)H_0+\frac{4}{9}\frac{\big(x+5\big)\big(5x+1\big)}{x+1}H_0^2
$$
$$
+\Bigg(\frac{16}{9}\big(x+9\big)-\frac{16}{3}\big(x+1\big)H_0\Bigg)H_1-\frac{64}{9}\big(x+1\big)H_1^2+\frac{16}{9}\big(x+1\big)H_{0,1}\Bigg)\zeta_2
$$
$$
+\Bigg(-\frac{8}{27}\frac{235x^2+404x+409}{x+1}-\frac{256}{9}\frac{x^2+1}{x+1}H_{-1}+\frac{8}{9}\frac{15x^2+22x+15}{x+1}H_0
$$
$$
-\frac{80}{9}\big(x+1\big)H_1\Bigg)\zeta_3+\frac{4}{9}\frac{131x^2+178x+131}{x+1}\zeta_4+\Bigg(\frac{1}{81}\big(-10999x-8399\big)
$$
$$
+\frac{64}{81}\frac{199x^2+174x+199}{x+1}H_{-1}-\frac{64}{9}\big(x+1\big)H_{-1}^2+\frac{128}{27}\frac{x^2+1}{x+1}H_{-1}^3\Bigg)H_0
$$
$$
+\Bigg(-\frac{2}{81}\frac{4179x^2+5255x+2868}{x+1}+\frac{32}{27}\frac{19x^2+18x+19}{x+1}H_{-1}-\frac{32}{9}\frac{x^2+1}{x+1}H_{-1}^2\Bigg)H_0^2
$$
$$
+\Bigg(-\frac{10}{81}\frac{177x^2+218x+105}{x+1}+\frac{64}{27}\frac{x^2+1}{x+1}H_{-1}\Bigg)H_0^3-\frac{1}{27}\frac{51x^2+70x+51}{x+1}H_0^4
$$
$$
+\Bigg(\frac{1}{27}\big(-3457x+1951\big)-\frac{16}{81}\big(593x+335\big)H_0-\frac{8}{27}\big(146x+71\big)H_0^2
$$
$$
-\frac{152}{27}\big(x+1\big)H_0^3\Bigg)H_1+\Bigg(-\frac{8}{9}\big(3x+55\big)-\frac{8}{9}\big(9x+1\big)H_0+\frac{4}{9}\big(x+1\big)H_0^2\Bigg)H_1^2
$$
$$
-\frac{64}{27}\big(x+1\big)H_0H_1^3+\Bigg(-\frac{64}{81}\frac{199x^2+174x+199}{x+1}+\frac{128}{9}\big(x+1\big)H_{-1}
$$
$$
-\frac{128}{9}\frac{x^2+1}{x+1}H_{-1}^2\Bigg)H_{0,-1}+\Bigg(\frac{4}{27}\big(251x+407\big)-\frac{512}{27}\frac{4x^2+3x+4}{x+1}H_{-1}
$$
$$
+\frac{16}{27}\big(10x+43\big)H_0+\frac{16}{3}\big(x+1\big)H_0^2+\Bigg(\frac{64}{9}\big(x-1\big)-\frac{80}{9}\big(x+1\big)H_0\Bigg)H_1
$$
$$
+\frac{64}{9}\big(x+1\big)H_1^2\Bigg)H_{0,1}+\frac{8}{9}\big(x+1\big)H_{0,1}^2+\Bigg(\frac{256}{9}\frac{x^2+1}{x+1}H_{-1}-\frac{128}{9}\big(x+1\big)\Bigg)H_{0,-1,-1}
$$

$$+\frac{512}{27}\frac{4x^2+3x+4}{x+1}H_{0,-1,1}+\left(-\frac{64}{27}\frac{19x^2+18x+19}{x+1}\right.$$
$$\left.+\frac{128}{9}\frac{x^2+1}{x+1}H_{-1}\right)H_{0,0,-1}+\left(\frac{4}{27}\frac{357x^2+130x+93}{x+1}-\frac{128}{9}\frac{x^2+1}{x+1}H_{-1}\right.$$
$$\left.-\frac{64}{9}(x+1)H_0+\frac{128}{9}(x+1)H_1\right)H_{0,0,1}+\frac{512}{27}\frac{4x^2+3x+4}{x+1}H_{0,1,-1}$$
$$+\left(-\frac{32}{9}(13x+1)+\frac{256}{9}\frac{x^2+1}{x+1}H_{-1}+\frac{16}{3}(x+1)H_0-\frac{32}{3}(x+1)H_1\right)H_{0,1,1}$$
$$+\frac{128}{9}\frac{x^2+1}{x+1}(-2H_{0,-1,-1,-1}-2H_{0,-1,1,1}-H_{0,0,-1,-1}+H_{0,0,-1,1}-H_{0,0,0,-1}$$
$$+H_{0,0,1,-1}-2H_{0,1,-1,1}-2H_{0,1,1,-1})+\frac{8}{9}\frac{21x^2+10x+21}{x+1}H_{0,0,0,1}$$
$$\left.-\frac{32}{9}\frac{7x^2+6x+7}{x+1}H_{0,0,1,1}\right]$$
$$+C_FT_F^2\left[-(2L_M^3+L_Q^3)\frac{32}{27}(x+1)+L_M^2\left[-\frac{32}{27}(11x-1)-\frac{32}{9}(x+1)H_0\right]\right.$$
$$+L_Q^2\left[\frac{32}{27}(14x+5)+\frac{64}{9}(x+1)H_0+\frac{32}{9}(x+1)H_1\right]-L_M\frac{992}{81}(x+1)$$
$$+L_Q\left[-\frac{32}{81}(187x+16)+\frac{128}{9}(x+1)\zeta_2-\frac{64}{27}(28x+13)H_0-\frac{32}{3}(x+1)H_0^2\right.$$
$$\left.+\left(-\frac{64}{27}(14x+5)-\frac{64}{9}(x+1)H_0\right)H_1-\frac{32}{9}(x+1)H_1^2-\frac{64}{9}(x+1)H_{0,1}\right]$$
$$+\frac{16}{729}(431x+323)-\frac{448}{27}(x+1)\zeta_3+\frac{64}{81}(6x-7)H_0+\frac{16}{81}(11x-1)H_0^2$$
$$\left.+\frac{16}{81}(x+1)H_0^3\right]+C_FN_FT_F^2\left[-(L_M^3+2L_Q^3)\frac{32}{27}(x+1)+L_Q^2\left[\frac{64}{27}(14x+5)\right.\right.$$
$$\left.+\frac{128}{9}(x+1)H_0+\frac{64}{9}(x+1)H_1\right]+L_M\left[\frac{32}{81}(5x-73)+\frac{32}{27}(11x-1)H_0\right.$$
$$\left.+\frac{16}{9}(x+1)H_0^2\right]+L_Q\left[-\frac{64}{81}(187x+16)+\frac{256}{9}(x+1)\zeta_2-\frac{128}{27}(28x+13)H_0\right.$$
$$-\frac{64}{3}(x+1)H_0^2+\left(-\frac{128}{27}(14x+5)-\frac{128}{9}(x+1)H_0\right)H_1-\frac{64}{9}(x+1)H_1^2$$
$$\left.-\frac{128}{9}(x+1)H_{0,1}\right]-\frac{64}{729}(161x+215)+\frac{256}{27}(x+1)\zeta_3+\frac{128}{81}(6x-7)H_0$$
$$\left.+\frac{32}{81}(11x-1)H_0^2+\frac{32}{81}(x+1)H_0^3\right]$$
$$+\frac{d^{abc}d^{abc}}{N_c}\frac{1}{2}L_Q\left[-\frac{800}{3}(x-1)+\left(-\frac{4}{3}(41x+67)-8\frac{(x+1)(4x^2-x+4)}{x}H_{-1}\right.\right.$$
$$+\frac{4}{3}(32x^2+27x+3)H_0-4(3x+5)H_0^2+\frac{8}{3}\frac{(x-1)(4x^2+7x+4)}{x}H_1$$
$$\left.-16(x-1)H_{0,-1}-16(x+1)H_{0,1}\right)\zeta_2+\left(\frac{32}{3}(5x^2+3)-32H_0\right)\zeta_3+10(5x+3)\zeta_4$$

$$
+\Biggl(\frac{4}{3}\bigl(9x+100\bigr)-\frac{104}{3}\bigl(x+1\bigr)H_{-1}-\frac{8}{3}\frac{\bigl(x+1\bigr)\bigl(4x^2-7x+4\bigr)}{x}H_{-1}^2\Biggr)H_0
$$
$$
+\Biggl(\frac{2}{3}\bigl(29x+38\bigr)+\frac{4}{3}\frac{\bigl(x+1\bigr)\bigl(8x^2-5x+8\bigr)}{x}H_{-1}\Biggr)H_0^2-\frac{4}{9}\bigl(8x^2+3\bigr)H_0^3
$$
$$
+\frac{2}{3}H_0^4+\Biggl(-\frac{364}{3}\bigl(x-1\bigr)+6\bigl(x-1\bigr)H_0^2\Biggr)H_1+\Biggl(\frac{104}{3}\bigl(x+1\bigr)-\frac{32}{3}\frac{3x^2+2}{x}H_0
$$
$$
+8\bigl(x-1\bigr)H_0^2+\frac{16}{3}\frac{\bigl(x+1\bigr)\bigl(4x^2-7x+4\bigr)}{x}H_{-1}\Biggr)H_{0,-1}+16\bigl(x-1\bigr)H_{0,-1}^2
$$
$$
+\Biggl(\frac{164}{3}\bigl(x+1\bigr)+\frac{32}{3}\frac{\bigl(x+1\bigr)\bigl(2x^2+x+2\bigr)}{x}H_{-1}-12\bigl(x-1\bigr)H_0
$$
$$
-4\bigl(x+1\bigr)H_0^2\Biggr)H_{0,1}+\Biggl(-\frac{16}{3}\frac{\bigl(x+1\bigr)\bigl(4x^2-7x+4\bigr)}{x}-32\bigl(x-1\bigr)H_0\Biggr)H_{0,-1,-1}
$$
$$
+\Biggl(-\frac{8}{3}\frac{8x^3-21x^2+3x-8}{x}-16\bigl(x-1\bigr)H_0\Biggr)H_{0,0,-1}
$$
$$
-\frac{32}{3}\frac{\bigl(x+1\bigr)\bigl(2x^2+x+2\bigr)}{x}H_{0,-1,1}+\Biggl(-\frac{8}{3}\bigl(8x^2+9x+3\bigr)+16\bigl(x+1\bigr)H_0\Biggr)H_{0,0,1}
$$
$$
-\frac{32}{3}\frac{\bigl(x+1\bigr)\bigl(2x^2+x+2\bigr)}{x}H_{0,1,-1}\Biggr]+\hat{C}_{q,3}^{\rm NS,(3)}(N_F)\Biggr\} \tag{2.68}
$$

Again, we used the short hand notation $H_{\vec{a}}(x) \equiv H_{\vec{a}}$ also here. The transformation of the Wilson coefficient to the $\overline{\rm MS}$ scheme for the heavy quark mass affects the massive OME at 3-loops and was given in Ref. [30]; the terms are the same in the unpolarized and polarized case.

The +-distribution of the Wilson coefficient also contains $1/(1-x)^2$-terms, cf. [30]. The explicit expressions for the Wilson coefficient $H_{q,3}^{\rm NS}(N_F+1)$ can be easily obtained from Eq. (2.6).

3 Numerical Results

In what follows, we will choose the factorization and renormalization scale $\mu^2 = Q^2$. We first study the behaviour of the massive and massless Wilson coefficients in the small and large x region and then give numerical illustrations in the whole x-region.

At small x, the pure massive Wilson coefficient behaves like

$$
L_{q,3}^{\rm NS}(N_F+1) - \hat{C}_{q,3}^{\rm NS}(N_F) \;\propto\; a_s^2\frac{2}{3}C_F T_F \ln^2(x) + a_s^3\left[\frac{16}{27}C_A C_F T_F - \frac{5}{9}C_F^2 T_F\right]\ln^4(x), \tag{3.1}
$$

while in the region $x \to 1$ one obtains[6]

$$
\begin{aligned}
L_{q,3}^{\rm NS}(N_F+1) - \hat{C}_{q,3}^{\rm NS}(N_F) \;\propto\;& a_s^2 C_F T_F\left[\frac{224}{27}+\frac{80}{9}L_M+\frac{8}{3}L_M^2\right]\left(\frac{1}{1-x}\right)_+ \\
&+a_s^3 C_F^2 T_F\left[\frac{448}{9}+\frac{160}{3}L_M+16L_M^2\right]\left(\frac{\ln^2(1-x)}{1-x}\right)_+ .
\end{aligned}
$$

[6]There is a typo in the second contribution to the $O(a_s^3)$ term of Eq. (3.2) in [49], which should be $\propto \ln(Q^2/m^2)$.

(3.2)

Likewise one obtains for $H_{q,3}^{\rm NS}(N_F+1)$ at small x

$$H_{q,3}^{\rm NS}(N_F+1) - C_{q,3}^{\rm NS}(N_F+1) \propto a_s^2 \frac{2}{3} C_F T_F \ln^2(x) + a_s^3 \left[\frac{16}{27} C_A C_F T_F - \frac{5}{9} C_F^2 T_F \right] \ln^4(x), \tag{3.3}$$

and in the region $x \to 1$

$$\begin{aligned} H_{q,3}^{\rm NS}(N_F+1) - C_{q,3}^{\rm NS}(N_F+1) \propto\ & a_s^2 C_F T_F \left[\frac{224}{27} + \frac{80}{9} L_M + \frac{8}{3} L_M^2 \right] \left(\frac{1}{1-x} \right)_+ \\ & + a_s^3 C_F^2 T_F \left[\frac{448}{9} + \frac{160}{3} L_M + 16 L_M^2 \right] \left(\frac{\ln^2(1-x)}{1-x} \right)_+ . \end{aligned} \tag{3.4}$$

The above results can be compared with the case of the massless Wilson coefficient $\hat{C}_{q,3}$ and $C_{q,3}$, respectively. The following dominant terms are found in the small and large x regions,

$$\hat{C}_{q,3}^{\rm NS,(2)}(N_F) \propto a_s^2 \frac{10}{3} C_F T_F \ln^2(x) \tag{3.5}$$

$$\hat{C}_{q,3}^{\rm NS,(3)}(N_F) \propto -a_s^3 \frac{2}{15} \frac{d^{abc} d^{abc}}{N_c} \ln^5(x) \tag{3.6}$$

$$C_{q,3}^{\rm NS,(1)}(N_F) \propto -a_s 2 C_F \ln(x) \tag{3.7}$$

$$C_{q,3}^{\rm NS,(2)}(N_F) \propto a_s^2 \left[\frac{7}{3} C_F^2 - 2 C_A C_F \right] \ln^3(x) \tag{3.8}$$

$$C_{q,3}^{\rm NS,(3)}(N_F) \propto a_s^3 \left[\frac{2}{5} C_A^2 C_F - \frac{29}{15} C_A C_F^2 + \frac{53}{30} C_F^3 - \frac{2}{15} \frac{d^{abc} d^{abc}}{N_c} N_F \right] \ln^5(x) \tag{3.9}$$

and

$$\hat{C}_{q,3}^{\rm NS,(2)}(N_F) \propto a_s^2 \frac{8}{3} C_F T_F \left(\frac{\ln^2(1-x)}{1-x} \right)_+ \tag{3.10}$$

$$\hat{C}_{q,3}^{\rm NS,(3)}(N_F) \propto a_s^3 \frac{80}{9} C_F^2 T_F \left(\frac{\ln^4(1-x)}{1-x} \right)_+ \tag{3.11}$$

$$C_{q,3}^{\rm NS,(1)}(N_F) \propto a_s 4 C_F \left(\frac{\ln(1-x)}{1-x} \right)_+ \tag{3.12}$$

$$C_{q,3}^{\rm NS,(2)}(N_F) \propto a_s^2 8 C_F^2 \left(\frac{\ln^3(1-x)}{1-x} \right)_+ \tag{3.13}$$

$$C_{q,3}^{\rm NS,(3)}(N_F) \propto a_s^3 8 C_F^3 \left(\frac{\ln^5(1-x)}{1-x} \right)_+ , \tag{3.14}$$

respectively.

Let us finally also consider the case $L_Q \neq 0$. Terms of this order have the following leading small and large x behaviour

$$\hat{C}_{q,3}^{\rm NS,(2)}(N_F) \propto -a_s^2 \frac{16}{3} C_F T_F L_Q \ln(x) \tag{3.15}$$

$$\hat{C}_{q,3}^{\rm NS,(3)}(N_F) \propto a_s^3 \frac{1}{3}\frac{d^{abc}d^{abc}}{N_c} L_Q \ln^4(x) \tag{3.16}$$

$$C_{q,3}^{\rm NS,(1)}(N_F) \propto a_s 2 C_F L_Q \tag{3.17}$$

$$C_{q,3}^{\rm NS,(2)}(N_F) \propto a_s^2 4 C_F \left[C_A - C_F\right] L_Q \ln^2(x) \tag{3.18}$$

$$C_{q,3}^{\rm NS,(3)}(N_F) \propto a_s^3 \left[-C_A^2 C_F + \frac{17}{3} C_A C_F^2 - \frac{11}{2} C_F^3 + \frac{1}{3}\frac{d^{abc}d^{abc}}{N_c} N_F\right] L_Q \ln^4(x) \tag{3.19}$$

and

$$\hat{C}_{q,3}^{\rm NS,(2)}(N_F) \propto a_s^2 \frac{16}{3} C_F T_F L_Q \left(\frac{\ln(1-x)}{1-x}\right)_+ \tag{3.20}$$

$$\hat{C}_{q,3}^{\rm NS,(3)}(N_F) \propto a_s^3 \frac{320}{9} C_F^2 T_F L_Q \left(\frac{\ln^3(1-x)}{1-x}\right)_+ \tag{3.21}$$

$$C_{q,3}^{\rm NS,(1)}(N_F) \propto a_s 4 C_F \left(\frac{1}{1-x}\right)_+ \tag{3.22}$$

$$C_{q,3}^{\rm NS,(2)}(N_F) \propto a_s^2 24 C_F^2 \left(\frac{\ln^2(1-x)}{1-x}\right)_+ \tag{3.23}$$

$$C_{q,3}^{\rm NS,(3)}(N_F) \propto a_s^3 40 C_F^3 L_Q \left(\frac{\ln^4(1-x)}{1-x}\right)_+ , \tag{3.24}$$

respectively, and are less singular than those for $L_Q = 0$.

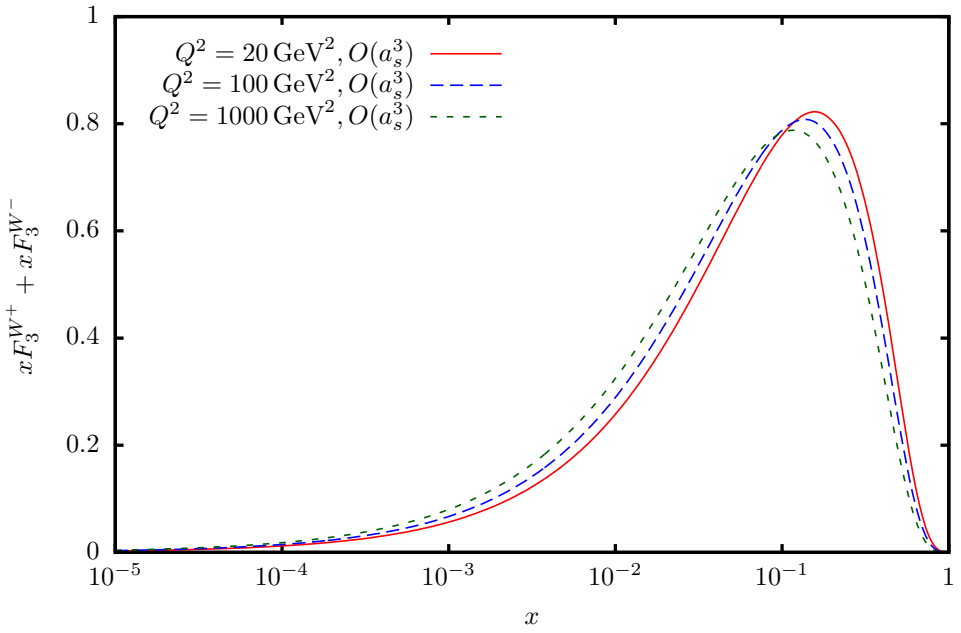

Figure 1: The corrections up to 3-loop order to the combination of the structure functions $xF_3^{W^+}(x,Q^2) + xF_3^{W^-}(x,Q^2)$ off a proton target, including both the massless and the charm contributions in the asymptotic approximation in the on-shell scheme for $m_c = 1.59$ GeV [17] as a function of x and Q^2. The parton distribution functions of Ref. [52] have been used with $\alpha_s(M_Z^2) = 0.1132$. These settings are the same in the subsequent Figures.

The small x behaviour can be compared with leading order predictions for the non-singlet

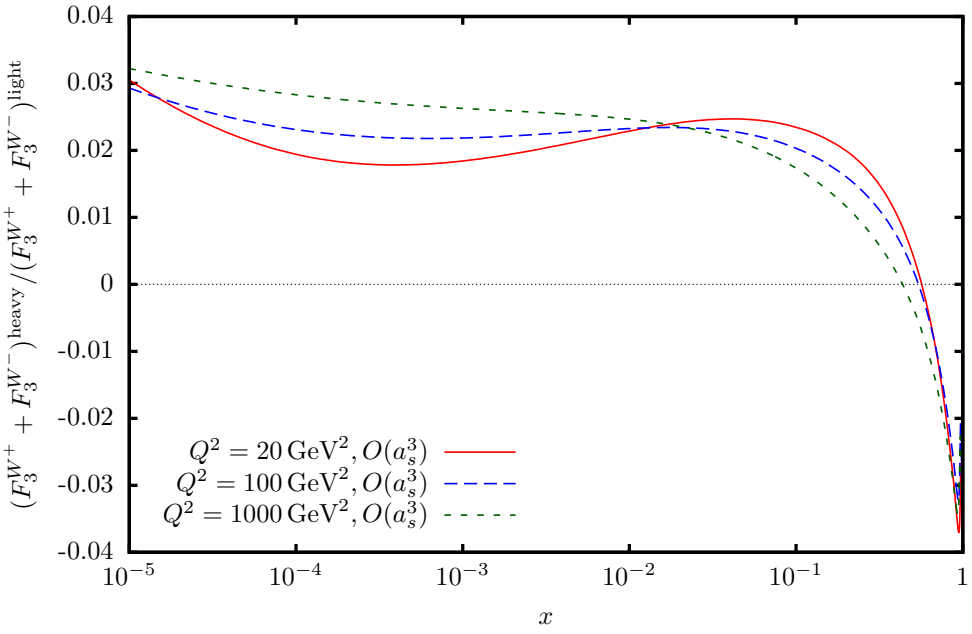

Figure 2: Ratio of the structure functions $xF_3^{W^+}(x,Q^2) + xF_3^{W^-}(x,Q^2)$ off a proton target up to 3-loop order for the charm contribution and the massless terms for three flavors.

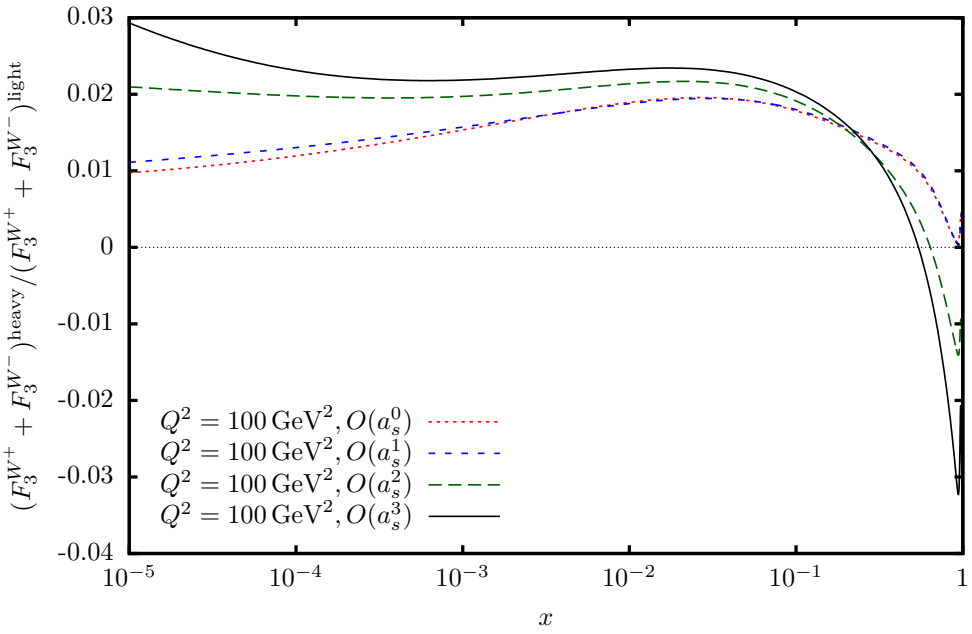

Figure 3: Ratio of the structure functions $xF_3^{W^+}(x,Q^2) + xF_3^{W^-}(x,Q^2)$ off a proton target up to 3-loop order for the charm contribution and the massless terms for three flavors from tree-level to $O(a_s^3)$ at $Q^2 = 100$ GeV^2.

evolution kernel in Refs. [50,51]. Indeed, both the massive and massless contributions follow the principle pattern $\sim c_k a_s^{k+1} \ln^{2k}(x)$. However, as is well known [51], less singular terms widely

cancel the numerical effect of these leading terms. For the large x terms the massless terms exhibit a stronger soft singularity than the massive ones.

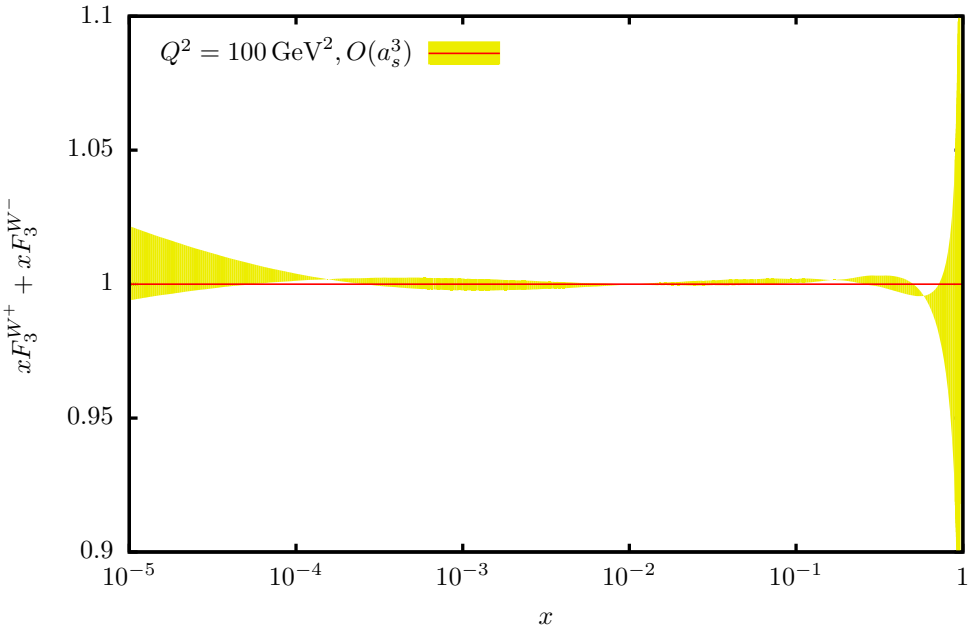

Figure 4: The ratio of the structure functions $xF_3^{W^+}(x,\mu^2) + xF_3^{W^-}(x,\mu^2)$ to $xF_3^{W^+}(x,Q^2) + xF_3^{W^-}(x,Q^2)$, varying $\mu^2 \in [Q^2/4, 4Q^2]$ at $O(a_s^3)$ and $Q^2 = 100$ GeV^2 as a function of x.

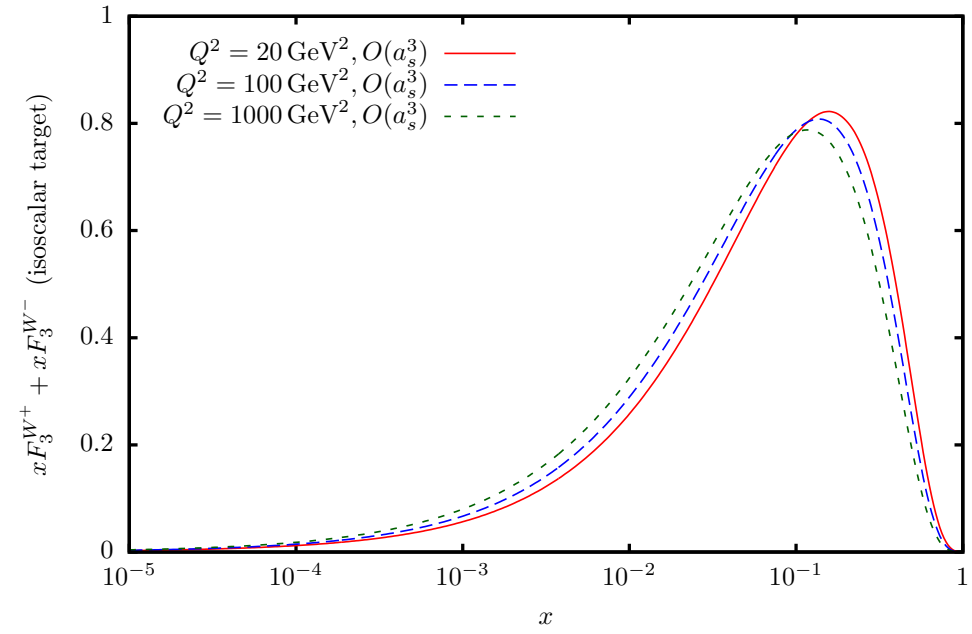

Figure 5: The corrections up to 3-loop order to the combination of the structure functions $xF_3^{W^+}(x,Q^2) + xF_3^{W^-}(x,Q^2)$ off a nucleon in an isoscalar target, including both the massless and charm contributions in the asymptotic approximation.

In Figure 1 we present the combination of structure functions $xF_3^{W^+-W^-,\rm NS}$ up to $O(a_s^3)$ at a proton target as a function of x and Q^2 up to 3-loop order for three massless flavors and charm in the asymptotic representation, assuming $m_c = 1.59$ GeV [53] in the on-shell scheme for mass renormalization and setting $\mu^2 = Q^2$. It shows valence-like scaling violations moving towards smaller values of x.

The effect of the charm contributions are illustrated in comparison to the purely massless ones up to $O(a_s^3)$ in Figure 2 evolving with Q^2. The contribution amounts to a correction of up to $+3\%$ in the small x region and to -3% in the large x region with some evolution in Q^2.

In Figure 3 we show a similar ratio as in Figure 2, but taken for each order of the perturbative corrections to $xF_3^{W^+}(x,\mu^2) + xF_3^{W^-}(x,\mu^2)$ separately at $Q^2 = 100$ GeV^2. In the small x region the corrections grow from 1% to 3%. At large values of x the relative corrections tend to become negative and do also amount to a few per cent. Figure 4 shows the remaining scale variations of the combination $xF_3^{W^+}(x,\mu^2) + xF_3^{W^-}(x,\mu^2)$ up to 3-loop order in the region $\mu^2 \in [Q^2/4, 4Q^2]$ normalized to the value at $\mu^2 = Q^2$ (yellow band) as a function of x for $Q^2 = 100$ GeV^2. The behaviour is overall flat with $\pm 1\%$ variations in the medium x-range and shows larger uncertainties at very low and large values of x. The behaviour is similar at other virtualities.

Figure 5 shows the combination of structure functions $xF_3^{W^+-W^-,\rm NS}$ up to $O(a_s^3)$ at a nucleon in an isoscalar target. The differences to the case of the proton target shown in Figure 1 turn out to be rather small in the case of this combination, which widely pronounces isoscalarity due to the present combination of currents, if $s_v \approx 0$.

4 The Gross-Llewellyn Smith Sum Rule

The Gross-Llewellyn Smith sum rule [54] refers to the first moment of the flavor non-singlet combination

$$\int_0^1 dx \left[F_3^{\bar{\nu}p}(x,Q^2) + F_3^{\nu p}(x,Q^2)\right] = 6 C_{\rm GLS}(\hat{a}_s), \tag{4.1}$$

with $\hat{a}_s = \alpha_s/\pi$ and idealized CKM mixing. The 1-loop [6, 7, 55, 56], 2-loop [57], 3-loop [58] and 4-loop QCD corrections [59, 60] in the massless case are given by

$$\begin{aligned} C_{\rm GLS}(\hat{a}_s), \;\; = \;\; & 1 - \hat{a}_s + \hat{a}_s^2(-4.58333 + 0.33333 N_F) + \hat{a}_s^3(-41.4399 + 7.74370 N_F - 0.17747 N_F^2) \\ & + \hat{a}_s^4(-479.448 + 140.796 N_F - 8.39702 N_F^2 + 0.10374 N_F^3) \;, \end{aligned} \tag{4.2}$$

choosing the renormalization scale $\mu^2 = Q^2$, for $SU(3)_c$. Here N_F denotes the number of active light flavors. The expression for general color factors was given in Ref. [59, 60]. Note that the QCD corrections to the Gross-Llewellyn Smith sum rule and to the polarized Bjorken sum rule [61] are identical up to $O(\hat{a}_s^2)$.

For the asymptotic massive corrections (2.4, 2.5) only the first moment of the massless Wilson coefficients $\hat{C}_{q,3}^{(2,3),\rm NS}(N_F)$ contributes, weighted by the first moments of the valence quark densities and the corresponding CKM matrix elements, since the first moments of the massive non-singlet OMEs vanish due to fermion number conservation. This also holds at higher order. Unlike the case of the polarized Bjorken sum rule [49], in the present case two massive Wilson coefficients contribute. One obtains

$$\begin{aligned} \int_0^1 dx \left[F_3^{\bar{\nu}p}(x,Q^2) + F_3^{\nu p}(x,Q^2)\right] \;\; = \;\; & 2\Big[(|V_{du}|^2 + |V_{su}|^2)\langle u_v\rangle + (|V_{dc}|^2 + |V_{du}|^2)\langle d_v\rangle\Big] \\ & \times C_{\rm GLS}(\hat{a}_s, N_F + 1) \end{aligned} \tag{4.3}$$

$$= \quad 2\,[2 \cdot 0.9999 + 0.9998]\, C_{\rm GLS}(\hat{a}_s, N_F + 1) \tag{4.4}$$

for the charm excitation with additional N_F light flavors. Here we assumed $s_v = 0$ and $\langle q_v \rangle = \int_0^1 dx q_v(x)$ denotes the first moment of a valence distribution. The CKM matrix elements currently imply a very small deviation from the factor 6 in (4.4) in the asymptotic case $Q^2 \gg m^2$ for proton targets. Very similar results are obtained for isoscalar targets. There are, in particular, no logarithmic corrections in the mass scales involved. The heavy quark just induces a shift $N_F \to N_F + 1$ w.r.t. the case of N_F light quarks only. Different results are obtained in the non-inclusive tagged-flavor case [13], which has been calculated to $O(\alpha_s^2)$. Here no inclusive structure functions are considered unlike the case in Ref. [14]. Corresponding power corrections in the tagged-flavor case were derived in Refs. [62, 63].

5 Conclusions

We calculated the heavy flavor non-singlet Wilson coefficients for the charged current structure function $xF_3^{W^+-W^-}(x,Q^2)$ to $O(\alpha_s^3)$ in the asymptotic region $Q^2 \gg m^2$. They can be expressed in terms of nested harmonic sums and polylogarithms. In contrast to the neutral current case, here, a second heavy flavor Wilson coefficient contributes, which describes the flavor excitation due to a $s \to c$ transition. The heavy flavor contributions to this combination of structure functions amounts up to the $O(\pm 3\%)$ for proton targets. Very similar results are obtained for deuteron targets, as the present combination approximately selects isoscalarity. In the small and large x regions the heavy flavor effects at 3-loop order are visible on top of those up to 2-loop orders by an enhancement and a depletion of $O(1\%)$, respectively, in the ratio to the 3-loop massless Wilson coefficient. This is below the present resolution reached at HERA, but may become of importance in high luminosity measurements at future colliders. The scale dependence reached for the non-singlet combination studied turns out to be widely flat. We also presented the leading terms in the heavy and light flavor Wilson coefficients at small and large values of the momentum fraction x.

In the asymptotic case $Q^2 \gg m^2$ the contribution of the massive Wilson coefficients to the Gross-Llewellyn Smith sum rule reduce to the replacement $N_F \to N_F + 1$ in the massless approximation. One has to note CKM-matrix effects here.

A Appendix

The massless Wilson coefficients and anomalous dimensions for $xF_3^{W^+}(x,Q^2) + xF_3^{W^+}(x,Q^2)$ contain a new color factor proportional to $d^{abc}d^{abc}$ ($= 40/3$ in QCD) [23, 43]. This color factor does not appear in the massive operator matrix elements at 3-loop order, which we would like to discuss in the following. Those terms, however, do arise in individual diagrams contributing to the OMEs but they cancel in the complete result. The cancellation can be seen as follows.

The color factor can appear when there are two separate fermion lines connected by three gluons. One fermion line connected to three gluons yields the color structure

$$\mathrm{Tr}[t^a t^b t^c] \quad = \quad \frac{T_F}{2}(i f^{abc} + d^{abc})\,. \tag{A.1}$$

Thus, two fermion lines connected by three individual gluon propagators produce the color structure

$$\mathrm{Tr}[t^a t^b t^c]\delta^{aa'}\delta^{bb'}\delta^{cc'}\mathrm{Tr}[t^{a'} t^{b'} t^{c'}] \quad = \quad \frac{T_F^2}{4}(-f^{abc}f^{abc} + d^{abc}d^{abc})\,. \tag{A.2}$$

For each such diagram there is a corresponding diagram with the fermion flow along the closed fermion loop reversed. An example of a pair of diagrams is given in Figure 6. The closed loop has to have three quark-gluon vertices in order to produce the color factor and therefore the loop must have three fermion propagators. Keeping the direction of the momenta fixed, the reversal of the fermion flow entails a change of the sign of the momentum $\not{p}_i$ in the numerator of each fermion propagator,

$$\frac{i(\not{p}_i + m)}{p_i^2 - m^2} \quad \to \quad \frac{i(-\not{p}_i + m)}{p_i^2 - m^2} \ . \tag{A.3}$$

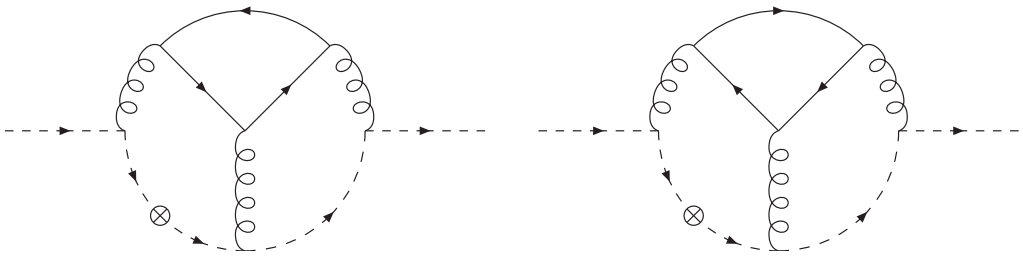

Figure 6: Example of a pair of diagrams which each contain a term proportional to the color factor $d^{abc}d^{abc}$.

This sign can be factored out since traces over an odd number of Dirac matrices vanish and yields a global factor (-1). Besides that, the reversal of the fermion flow also reverses the order of the color generators $t^{a'}t^{b'}t^{c'}$ in Eq. (A.2) which flips the sign in front of the $f^{abc}f^{abc}$ term, but leaves the $d^{abc}d^{abc}$ term unchanged. We see that each pair of such diagrams has exactly the same integrand, but the sign in front of the $d^{abc}d^{abc}$ color factor is changed. Therefore, this color factor cancels in the sum for each pair of diagrams.

Acknowledgment. We would like to thank J. Ablinger, K. Chetyrkin, M. Round, A. Vogt, and F. Wißbrock for discussions. This work was supported in part by the European Commission through contract PITN-GA-2012-316704 (HIGGSTOOLS) and Austrian Science Fund (FWF) grant SFB F50 (F5009-N15). The Feynman diagrams were drawn using `Axodraw` [64].

References

[1] F. Eisele, Rept. Prog. Phys. **49** (1986) 233.

[2] M. Diemoz, F. Ferroni and E. Longo, Phys. Rept. **130** (1986) 293.

[3] N. Schmitz, Neutrinophysik, (Teubner, Stuttgart, 1997).

[4] J. Blümlein, H. Böttcher and A. Guffanti, Nucl. Phys. B **774** (2007) 182 [hep-ph/0607200]; Nucl. Phys. Proc. Suppl. **135** (2004) 152 [hep-ph/0407089].

[5] J. Blümlein and A. Vogt, Phys. Rev. D **58** (1998) 014020 [hep-ph/9712546].

[6] W. A. Bardeen, A. J. Buras, D. W. Duke and T. Muta, Phys. Rev. D **18** (1978) 3998.

[7] W. Furmanski and R. Petronzio, Z. Phys. C **11** (1982) 293 and references therein.

[8] M. Glück, S. Kretzer and E. Reya, Phys. Lett. B **398** (1997) 381 [Erratum: Phys. Lett. B **405** (1997) 392] [hep-ph/9701364].

[9] J. Blümlein, A. Hasselhuhn, P. Kovacikova and S. Moch, Phys. Lett. B **700** (2011) 294 [arXiv:1104.3449 [hep-ph]].

[10] T. Gottschalk, Phys. Rev. D **23** (1981) 56.

[11] E. B. Zijlstra and W. L. van Neerven, Phys. Lett. B **297** (1992) 377.

[12] S. Moch and J.A.M. Vermaseren, Nucl. Phys. B **573** (2000) 853 [hep-ph/9912355].

[13] M. Buza and W. L. van Neerven, Nucl. Phys. B **500** (1997) 301 [hep-ph/9702242].

[14] J. Blümlein, A. Hasselhuhn and T. Pfoh, Nucl. Phys. B **881** (2014) 1 [arXiv:1401.4352 [hep-ph]].

[15] A. Hasselhuhn, 3-Loop Contributions to Heavy Flavor Wilson Coefficients of Neutral and Charged Current DIS, PhD Thesis TU Dortmund, 2013, DESY-THESIS-2013-050.

[16] M. Buza, Y. Matiounine, J. Smith, R. Migneron and W. L. van Neerven, Nucl. Phys. B **472** (1996) 611 [hep-ph/9601302].

[17] S. Alekhin, J. Blümlein, L. Caminadac, K. Lipka, K. Lohwasser, S. Moch, R. Petti and R. Placakyte, Phys. Rev. D **91** (2015) 9, 094002 [arXiv:1404.6469 [hep-ph]].

[18] K.A. Olive et al. (Particle Data Group), Chin. Phys. C, 38, 090001 (2014).

[19] D. M. Kaplan [MAP and MICE Collaborations], EPJ Web Conf. **95** (2015) 03019 [arXiv:1412.3487 [physics.acc-ph]].

[20] J. L. Abelleira Fernandez *et al.* [LHeC Study Group Collaboration], J. Phys. G **39** (2012) 075001 [arXiv:1206.2913 [physics.acc-ph]].

[21] D. Boer, M. Diehl, R. Milner, R. Venugopalan, W. Vogelsang, D. Kaplan, H. Montgomery, S. Vigdor *et al.*, arXiv:1108.1713 [nucl-th];
A. Accardi, J. L. Albacete, M. Anselmino, N. Armesto, E. C. Aschenauer, A. Bacchetta, D. Boer, W. Brooks *et al.*, arXiv:1212.1701 [nucl-ex].

[22] S. Bethke *et al.*, Workshop on Precision Measurements of α_s, arXiv:1110.0016 [hep-ph];
S. Moch, S. Weinzierl, *et al.*, High precision fundamental constants at the TeV scale, arXiv:1405.4781 [hep-ph].

[23] S. Moch, J.A.M. Vermaseren and A. Vogt, Nucl. Phys. B **813** (2009) 220 [arXiv:0812.4168 [hep-ph]].

[24] A. Arbuzov, D.Y. Bardin, J. Blümlein, L. Kalinovskaya and T. Riemann, Comput. Phys. Commun. **94** (1996) 128 [hep-ph/9511434];
J. Blümlein, M. Klein, T. Naumann and T. Riemann, PHE-88-01.

[25] J. Blümlein, Prog. Part. Nucl. Phys. **69** (2013) 28 [arXiv:1208.6087 [hep-ph]].

[26] N. Cabibbo, Phys. Rev. Lett. **10** (1963) 531.

[27] M. Kobayashi and T. Maskawa, Prog. Theor. Phys. **49** (1973) 652.

[28] W. L. van Neerven and A. Vogt, Nucl. Phys. B **588** (2000) 345 [hep-ph/0006154].

[29] I. Bierenbaum, J. Blümlein and S. Klein, Nucl. Phys. B **820** (2009) 417 [arXiv:0904.3563 [hep-ph]].

[30] J. Ablinger, A. Behring, J. Blümlein, A. De Freitas, A. Hasselhuhn, A. von Manteuffel, M. Round, C. Schneider, and F. Wißbrock, Nucl. Phys. B **886** (2014) 733 [arXiv:1406.4654 [hep-ph]].

[31] J. Lagrange, Nouvelles recherches sur la nature et la propagation du son, Miscellanea Taurinensis, t. II, 1760-61; Oeuvres t. I, p. 263;
C.F. Gauss, Theoria attractionis corporum sphaeroidicorum ellipticorum homogeneorum methodo novo tractate, Commentationes societas scientiarum Gottingensis recentiores, Vol III, 1813, Werke Bd. **V** pp. 5-7;
G. Green, Essay on the Mathematical Theory of Electricity and Magnetism, Nottingham, 1828 [Green Papers, pp. 1-115];
M. Ostrogradski, Mem. Ac. Sci. St. Peters., **6**, (1831) 39;
K. G. Chetyrkin, A. L. Kataev and F. V. Tkachov, Nucl. Phys. B **174** (1980) 345.

[32] A. von Manteuffel and C. Studerus, arXiv:1201.4330 [hep-ph];
C. Studerus, Comput. Phys. Commun. **181** (2010) 1293 [arXiv:0912.2546 [physics.comp-ph]].

[33] R.H. Lewis, Computer Algebra System `Fermat`, `http://home.bway.net/lewis`.

[34] C.W. Bauer, A. Frink and R. Kreckel, Symbolic Computation **33** (2002) 1, cs/0004015 [cs-sc].

[35] C. Schneider, Sém. Lothar. Combin. **56** (2007) 1, article B56b.

[36] C. Schneider, Computer Algebra in Quantum Field Theory: Integration, Summation and Special Functions Texts and Monographs in Symbolic Computation eds. C. Schneider and J. Blümlein (Springer, Wien, 2013) 325, arXiv:1304.4134 [cs.SC].

[37] J. Ablinger, J. Blümlein, S. Klein and C. Schneider, Nucl. Phys. Proc. Suppl. **205-206** (2010) 110 [arXiv:1006.4797 [math-ph]];
J. Blümlein, A. Hasselhuhn and C. Schneider, PoS **RADCOR2011** (2011) 032 [arXiv:1202.4303 [math-ph]];
C. Schneider, Proc. of ACAT 2013, J. Phys. Conf. Ser. 523 (2014) 012037, pp. 1 [arXiv:1310.0160 [cs.SC]].

[38] C. Schneider, Advances in Applied Math **34**(4) (2005) 740, D. Bressoud (ed.).
J. Ablinger, J. Blümlein, M. Round and C. Schneider, PoS **LL2012** (2012) 050 [arXiv:1210.1685 [cs.SC]];
M. Round et al., in preparation.

[39] J. Ablinger, PoS **LL2014** (2014) 019; Computer Algebra Algorithms for Special Functions in Particle Physics, Ph.D. Thesis, J. Kepler University Linz, 2012, arXiv:1305.0687 [math-ph]; A Computer Algebra Toolbox for Harmonic Sums Related to Particle Physics, Diploma Thesis, J. Kepler University Linz, 2009, arXiv:1011.1176 [math-ph];
J. Ablinger, J. Blümlein and C. Schneider, J. Math. Phys. **52** (2011) 102301 [arXiv:1105.6063 [math-ph]]; J. Ablinger, J. Blümlein and C. Schneider, J. Math. Phys. **54** (2013) 082301 [arXiv:1302.0378 [math-ph]];
J. Ablinger, J. Blümlein, C. G. Raab and C. Schneider, J. Math. Phys. **55** (2014) 112301 [arXiv:1407.1822 [hep-th]].

[40] J.A.M. Vermaseren, Int. J. Mod. Phys. A **14** (1999) 2037[hep-ph/9806280];
J. Blümlein and S. Kurth, Phys. Rev. D **60** (1999) 014018 [hep-ph/9810241].

[41] J. Blümlein, D. J. Broadhurst and J.A.M. Vermaseren, Comput. Phys. Commun. **181** (2010) 582 [arXiv:0907.2557 [math-ph]].

[42] L. Lewin, Dilogarithms and associated functions, (Macdonald, London, 1958); Polylogarithms and associated functions, (North Holland, New York, 1981).

[43] S. A. Larin, T. van Ritbergen and J.A.M. Vermaseren, Nucl. Phys. B **427** (1994) 41;
S. A. Larin, P. Nogueira, T. van Ritbergen and J.A.M. Vermaseren, Nucl. Phys. B **492** (1997) 338 [hep-ph/9605317];
A. Retey and J.A.M. Vermaseren, Nucl. Phys. B **604** (2001) 281 [hep-ph/0007294];
J. Blümlein and J.A.M. Vermaseren, Phys. Lett. B **606** (2005) 130 [hep-ph/0411111];
S. Moch, J.A.M. Vermaseren and A. Vogt, Nucl. Phys. B **688** (2004) 101 [hep-ph/0403192].

[44] J. Blümlein, Comput. Phys. Commun. **180** (2009) 2218 [arXiv:0901.3106 [hep-ph]].

[45] J. Blümlein, in : Proceedings of the Workshop Motives, Quantum Field Theory, and Pseudodifferential Operators, Clay Mathematics Institute, Boston University, June 2–13, 2008, Clay Mathematics Proceedings **12** (2010) 167, Eds. A. Carey, D. Ellwood, S. Paycha, S. Rosenberg, arXiv:0901.0837 [math-ph].

[46] J. Blümlein, Comput. Phys. Commun. **133** (2000) 76 [hep-ph/0003100];
J. Blümlein and S. O. Moch, Phys. Lett. B **614** (2005) 53 [hep-ph/0503188].

[47] E. Remiddi and J.A.M. Vermaseren, Int. J. Mod. Phys. A **15** (2000) 725 [hep-ph/9905237].

[48] J. Blümlein, Comput. Phys. Commun. **159** (2004) 19 [hep-ph/0311046].

[49] A. Behring, J. Blümlein, A. De Freitas, A. von Manteuffel and C. Schneider, Nucl. Phys. B **897** (2015) 612 [arXiv:1504.08217 [hep-ph]].

[50] R. Kirschner and L.N. Lipatov, Nucl. Phys. B **213** (1983) 122.

[51] J. Blümlein and A. Vogt, Phys. Lett. B **370** (1996) 149 [hep-ph/9510410]; Acta Phys. Polon. B **27** (1996) 1309 [hep-ph/9603450].

[52] S. Alekhin, J. Blümlein and S. Moch, Phys. Rev. D **89** (2014) 054028 [arXiv:1310.3059 [hep-ph]].

[53] S. Alekhin, J. Blümlein, K. Daum, K. Lipka and S. Moch, Phys. Lett. B **720** (2013) 172 [arXiv:1212.2355 [hep-ph]].

[54] D. J. Gross and C. H. Llewellyn Smith, Nucl. Phys. B **14** (1969) 337.

[55] G. Altarelli, R. K. Ellis and G. Martinelli, Nucl. Phys. B **143** (1978) 521, Erratum: Nucl. Phys. B **146** (1978) 544.

[56] B. Humpert and W. L. van Neerven, Nucl. Phys. B **184** (1981) 225.

[57] S. G. Gorishnii and S. A. Larin, Phys. Lett. B **172** (1986) 109.

[58] S. A. Larin and J.A.M. Vermaseren, Phys. Lett. B **259** (1991) 345.

[59] P. A. Baikov, K. G. Chetyrkin, J. H. Kühn and J. Rittinger, Phys. Lett. B **714** (2012) 62 [arXiv:1206.1288 [hep-ph]].

[60] P. A. Baikov, K. G. Chetyrkin and J. H. Kühn, Phys. Rev. Lett. **104** (2010) 132004 [arXiv:1001.3606 [hep-ph]].

[61] J. D. Bjorken, Phys. Rev. D **1** (1970) 1376.

[62] J. Blümlein and W. L. van Neerven, Phys. Lett. B **450** (1999) 417 [hep-ph/9811351].

[63] W.L. van Neerven, in : Proceedings of the Workshop Hadron Physics: effctive theories of low-energy QCD, Coimbra, Portugal, 1999, AIP Conf.Proc. **508** (2000) pp. 162, Eds. A.H. Blin, B. Hiller, M.C. Ruivo, C.A. de Sousa, E. van Beveren [hep-ph/9910356].

[64] J.A.M. Vermaseren, Comput. Phys. Commun. **83** (1994) 45.